MET.O.14

METEOROLOGICAL OFFICE
BOUNDARY LAYER RESEARCH BRANCH
TURBULENCE & DIFFUSION NOTE

T.D.N. No. 153

Estimation of Fluxes from Routine Meteorological Data

by

Wang Jiemin*

The Institute of Plateau Atmospheric Physics
Chinese Academy of Sciences
Lanzhou, China.

*This work was carried out at the Boundary Layer Branch, Meteorological Office, U.K.

Estimation of Fluxes from Routine Meteorological Data

1. Introduction

Estimation of surface fluxes is essential for determining atmospheric stability which is in turn very important for air pollution modelling. Among the surface fluxes, the sensible heat flux H and the momentum flux, normally represented by the friction velocity U*, predominate. These fluxes can be measured either by the eddy correlation method, or less directly by wind and temperature profile measurements combined with empirical universal functions based on similarity theory. Often, none of these measurements is available, and it is necessary to give rough estimates through the use of standard meteorological observations of cloud, temperature, humidity, wind and precipitation.

The present study concerns this estimation. Particular attention was paid to two difficult points in this study:

(a) The estimation of net radiation Rn from solar elevation and cloud information;

(b) The estimation of the sensible heat flux H and the latent heat flux LE by the resistance method which involves the estimation of surface resistances.

For a uniform, horizontal land surface the balance of incoming and outgoing energy is governed by the equation

$$R_n = H + LE + G \qquad (1)$$

where G is the downward flux of heat into the soil. During day time, solar radiation is the main source of the net radiation. A part of the incoming energy is reflected back into space from the surface, but long-wave radiation from the ground, clouds and the atmosphere also contribute to the

net radiation flux. During night time, cooling of the surface and long-wave radiation from clouds and the atmosphere determine the net radiation. R_n is much larger and more changeable during the day than at night. This paper focuses upon the day-time situation. The way the available energy is partitioned into sensible, latent and soil heat fluxes depends on several factors, such as soil type, vegetation, and the state of the ground. This partioning will be estimated using Monteith's (1965) formula, after inferring the surface resistances. Then, the implied friction velocity u* can be obtained through an iterative procedure.

Comparison of these fluxes with independent data is deemed satisfactory and encourages the belief that the method is useful in practical applications, being not only reasonably accurate but sufficiently simple to be used with a hand-held programmable calculator.

2. Net Radiation Estimation

During day time the net radiation is directly related to the incident solar radiation at the earth's surface. Clearly it is a function of many variables. Here we consider the most important, namely solar elevation and cloud cover. (Lumb, 1964; Smith and Hunt, 1978; Nielson et al, 1981). Normally net radiation is calculated by a semi-empirical equation, such as

$$R_n = A_0 + A_1 S + A_2 S^2 + A_3 S^3 \qquad (2)$$

where $S = \sin\theta$. θ is the solar elevation, which is related to the latitude O of the station, (Julian) day number n of the year and the local time t. According to the standard formula,

$$S = \sin\theta = \sin\phi \sin A + \cos\phi \cos A \cos \frac{2\pi}{24} (t-12) \qquad (3)$$

where

$$A = 23.3 \sin\left[\frac{2\pi\,(n - 81)}{N}\right] \qquad (4)$$

A is the solar latitude (the latitude at which the sun is overhead). N, the number of days in the year (365 or 366). For the southern hemisphere equation (4) should be modified by changing 81 to 264.

The problem is to evaluate empirically the coefficients of equation (2), $A_0 - A_3$, which are mainly related to cloud cover.

Cloud information from standard meteorological stations is reported at the beginning of the hour and consists of the total amount and the amount and type at each of the three standard levels - low, medium, and high. Cloud amount is given in eighths (oktas) of the sky covered, with a ninth category associated with thick overcast clouds. There are ten classes of cloud type. Cloud data are however not as simple or as precise as other routine meteorological data. Therefore for practical purposes, both in evaluating the coefficients of equations (2) and in the estimation of net radiation, cloud data will be grouped and simplified. Lumb (1964) grouped the data mainly according to cloud type, into nine categories and presented nine sets of coefficients for an equation similar to (2). Nielson et al (1981) divided the data into nine different classes, mainly according to the total amount (except high cloud), and presented the associated coefficients of equation (2) for each okta.

Based on the analysis of Cardington data, which were collected during a micro-meteorological experiment held in March 1976 - March 1977, we conclude that the grouping of the cloud state can be much simpler, requiring only two classes. The following points lead to this conclusion:

(a) The ten types of clouds fall into three basic categories: Cirrus, Stratiform and Cumuliform. Cirrus (Ci, Cc and Cs), consisting of mainly ice crystals, is semi-transparent. It has little effect on radiation. Cirrus always appears at high altitudes.

(b) When cumuliform cloud is present the day is normally "partly cloudy", and there are breaks in the sky. The presence of cumulus in the lower layers over land implies that there is enough surface heating to generate it. Any cloud layers above the cumulus are normally thin. The alternately illuminated and shaded surfaces seem to receive almost as much sunshine as with clear skies. Moreover, data show that when there are only 1-2 oktas of cumuliform clouds the net radiation may be greater than when the sky is clear (Smith and Hunt, 1978). The reasons are probably that the high 'walls' of cumuliform clouds are good reflectors of downward radiation, and that cumulus is often associated with clear polar maritime air.

(c) Any practical method should be based on data that would be readily available. Routine reports of cloud information, although apparently complicated, are still very limited. As noted above the cloud observation is taken at the beginning of the hour. But the net radiation reported is the hourly mean of readings taken every one or two minutes. This is usually not satisfactory since the cloud cover can change completely within an hour. Also, since the observations are taken from the ground, any cloud in the higher layer that cannot be seen is not recorded. The three-layer cloud reports could omit some sub-layers. And the thickness of cloud is not measured, although this will obviously have a large effect on the results. Such deficiencies of cloud information cause severe limitations for the modelling prediction of the net radiation. From

the data analysis shown later it is clear that it would be a misleading approach to attempt to group the cloud state into more finely partitioned classes.

Fig 1 and 2 give two examples of the cloud-radiation plot. Fig 1 shows the time variation of R_n in a normal 'partly cloudy' day. It is clear that the radiation values at low solar elevation, particularly during night time, are small and rather steady. On the other hand at most hours of the day time the radiation value fluctuates, sometimes violently. The cloud reports and the hourly mean values of R_n are shown at the top of the Figure.

Fig 2 shows an example of scatter plot of net radiation against solar elevation under the two extreme cloud states: clear sky (including a few situations of total amount ≤ 2) and overcast (total amount ≥ 7, not counting high clouds). It is based on Cardington data from Mar - Aug 1976, which included 20 clear days. The points are very scattered. Even for the clear days, when there was almost no cloud reported during the whole day, the range of observed R_n is still more than 100 W/m^2 at any specified solar elevation. Scatter is even wider on the overcast days. Fig 2 shows that the two areas of points covering the two extreme cloud states adjoin and even overlap each other at low solar elevation. This figure again shows that it would not be very meaningful to group the cloud states into very fine classes. Other important factors presumably associated with atmospheric turbidity and state of ground, have yet to be identified.

In fact, it is clear from the Cardington data analysis that when the total cloud amount is 3-6 oktas (including high cloud = 7-8 oktas) the observed values of radiation are scattered predominantly within the range of the points for the clear sky situation, as can be seen by comparing Fig 3 with Fig 2. Based on this study the model was developed as follows:

Only two conditions for the state of cloud cover are considered:

I. Total amount $\leq$ 6 oktas, including high cloud $C_H \leq 8$ oktas.

II. Total amount $\geq$ 7 oktas, not counting C_H.

The coefficients of equation (2), based on the analysis of Cardington data, 1976, are shown in Table 1.

Table 1

Cloud condition	A_o	A_1	A_2	A_3
I	-45.0	102.5	742.2	-172.1
II	6.2	41.6	155.9	99.6

Figs 3 and 4 show the comparison between observed and calculated results obtained by using the model above. Fig 3 is a scatter plot of radiation at all observation times at Cardington during the period Apr - Aug 1976. It consists of 52 days data, totalling over 700 hours. Unreliable values were excluded; those mostly refer to situations with rain or fog. Curves I and II presented in the figure are equation (2) for cloud conditions I and II respectively. It is seen from Fig 3 that at high solar elevation the net radiation for cloud condition I is much higher than that for condition II, as would be expected. In contrast, at low solar

elevation, in the early morning and late afternoon, the radiation for condition II is higher. This is due to the contribution of long-wave radiation from the cloud.

The points scatter round the 45° line in Fig 4. The correlation between observed and modelling values is very good ($r = 0.95$).

It has been noted that, as shown in Fig 2, the points are widely scattered even in clear sky situations. This is not altogether surprising. As mentioned earlier, in addition to the error of observation there are still many other variables affecting the surface net radiation, e.g. the number of aerosol particles in the air associated in part with the state of air pollution. Unfortunately there are few data on atmospheric turbidity. Visibility might not provide a good criterion on which to supplement judgement for this purpose since it is only a property of the lowest layer of the atmosphere. Cardington data show that in late June to the beginning of July there were seven successive clear days; the net radiation at this period was smaller (50–100 Wm^{-2}) than that of the clear days in March, April and August (at the same solar elevation) although the visibility was better for many hours.

In order to evaluate the generality of the model derived above it has been tested against several independent data sets. The results are shown in Figs 5–14.

Figs 5–8 show the comparison of the model with two other independent Cardington experiments held in June, 1982, and Apr – May 1983, respectively. The agreement is reasonable. The variation of R_n in a typical "partly cloudy" day (cloud condition I) in the 1983 experiment is shown in Fig 1, along with the hourly average and modelling values.

Figs 9–10 show the comparison for a data set from Kew Observatory in 1978. The calculated value is slightly lower at high solar elevation. Even so the model works well ($r = 0.94$).

Cardington and Kew may represent the situation in England and even in some European countries, where the ground is covered by short grass. For stations with a quite different ground state (e.g. sparse grass or bare ground or with some other cover) the albedo may be quite different, and some parts of the model should be modified.

Figs 11–12 show the results for Wangara data (Clarke et al, 1971). The Wangara experiment was held in the winter of 1967, Hay, Australia, where there was almost no vegetation. The coefficients of the modelling equation (2) were different, as shown in Table 2:

Table 2

Cloud condition	A_0	A_1	A_2	A_3
I	-45.8	269.0	830.0	-400.0
II	-11.3	133.7	159.0	125.5

The clouds are grouped into two classes as before. It can be seen that the radiation is much stronger than in England.

The Wangara model (Table 2) was tried against the data set from another experiment held in Australia – the 'ITCE', which was held in Conargo in the summer of 1976 (Garratt et al, 1979). Because of the shortage of cloud reports (only three times a day), only seven days were chosen for comparison. The results are shown in Figs 13–14. There is an

apparent feature in the 'ITCE' day time radiation: on clear days (cloud ≤ 2), at the same solar elevation, the net radiation in the morning is higher (~20%) than that in the afternoon. This may be related to the much lower surface layer temperature in the morning.

Based on the analysis above it may be concluded that the semi-empirical equation (2) can be used for estimating net radiation. The coefficients of the equation are mainly related to the cloud cover. For normal situations, grouping the cloud states into only two classes is adequate. For stations with quite different ground state the coefficients should be determined afresh.

3. The Monteith formula

Monteith (1965) presented a general formula for the latent heat flux within the atmospheric surface layer above a vegetated surface. The formula uses the concept of surface resistance, which, in fact, expresses a combination of the energy balance equation (1), the relationships between fluxes and gradients of mean quantities and an a priori evaluation of surface conditions. A short review of the method is now given which will help in the later analysis.

The resistance method, widely used by plant physiologists, is based on an analogy with Ohm's law. The general form is

$$\text{Flux} = \frac{\text{Potential difference}}{\text{Resistance}}$$

Depending on which quantity the flux refers to, the potential difference corresponds to the appropriate mean field parameter. Thus, for momentum flux (here we consider the square of the friction velocity, U^{*2}), the

potential difference refers to wind speed difference (Δu); for sensible heat flux (H), the temperature difference (ΔT); for latent heat flux (LE), the water vapour pressure difference (Δe):

$$U_*^2 = \frac{\Delta u}{r_m} = \frac{U(Z_2) - U(Z_1)}{r_m} \qquad (5)$$

$$H = \frac{-\Delta T}{r_h} \cdot \rho C_p = \frac{T(Z_1) - T(Z_2)}{r_h} \rho C_p \qquad (6)$$

$$LE = \frac{-\Delta e}{r_w} \cdot \frac{\rho C_p}{\gamma} = \frac{e(Z_1) - e(Z_2)}{r_w} \cdot \frac{\rho C_p}{\gamma} \qquad (7)$$

where Z_1, Z_2 refer the heights at which the appropriate parameter is measured; ρ, the density of air; C_p, the specific heat of air at constant pressure; γ, the so-called psychrometric parameter, which varies only slowly with temperature; r_m, r_h and r_w are the resistances for the transfer of momentum, sensible heat and latent heat respectively, from height Z_1 to Z_2.

The meaning of these resistances can be seen more clearly with the help of the familiar flux-gradient relationships:

$$\frac{\partial U}{\partial Z} = \frac{U_*}{kZ} \phi_m(\zeta) \qquad (8)$$

$$\frac{\partial T}{\partial Z} = \frac{-T_*}{kZ} \phi_H(\zeta) \qquad (9)$$

$$\frac{\partial \chi}{\partial z} = \frac{-\chi^*}{kz}\,\phi_w(\zeta) \qquad (10)$$

where $\phi_m(\zeta)$, $\phi_H(\zeta)$ and $\phi_w(\zeta)$ are the similarity functions for momentum, heat and water vapour, which have been expressed empirically by many authors (see, e.g. Dyer and Hicks, 1970). $\zeta = z/L$ (L is the Monin-Obukhov length). K is the von Karman constant, χ is the absolute humidity, and T^* and χ^* are two scaling parameters defined by

$$H = \rho C_p\, U^*\, T^* \qquad (11)$$

$$E = U^*\, \chi^* \qquad (12)$$

If (8) - (10) are integrated between heights z_1 and z_2 and compared with (5) - (7), it follows that:

$$r_m = \frac{1}{kU^*}\int_{z_1}^{z_2}\frac{\phi_m(\zeta)}{z}\,dz = \frac{1}{kU^*}\,\psi_m(z_1, z_2, L) \qquad (13)$$

$$r_h = \frac{1}{kU^*}\int_{z_1}^{z_2}\frac{\phi_H(\zeta)}{z}\,dz = \frac{1}{kU^*}\,\psi_H(z_1, z_2, L) \qquad (14)$$

$$r_w = \frac{1}{kU^*}\int_{z_1}^{z_2}\frac{\phi_w(\zeta)}{z}\,dz = \frac{1}{kU^*}\,\psi_w(z_1, z_2, L) \qquad (15)$$

where ψ_m, ψ_H and ψ_w are the so called integrated similarity functions. It is commonly accepted that $\phi_H(\zeta) = \phi_w(\zeta)$, so that $\psi_H = \psi_w$, and $r_h = r_w$. Since the ψ's are functions of atmospheric stability (defined by L) the resistances r_m, r_h (r_w) are governed by atmospheric turbulence and are

therefore named aerodynamic resistances. If the wind is measured at a height Z_u, and the temperature and humidity are measured at height Z_T, then, in the simplest situation with neutral stratification and a roughness length Z_o, we have

$$r_m = \frac{1}{kU_*} \cdot \ln \frac{Z_u}{Z_o} = \frac{1}{k^2 U(Z_u)} \cdot \left(\ln \frac{Z_u}{Z_o}\right)^2 \qquad (16)$$

$$r_a = r_h = r_w = \frac{1}{k^2 U(Z_u)} \left(\ln \frac{Z_u}{Z_o} \cdot \ln \frac{Z_T}{Z_o}\right) \qquad (17)$$

Methods of estimating r_a for different atmosphere stabilities will be discussed later.

Rewriting (6) and (7),

$$H = \frac{T(Z_o) - T(Z_T)}{r_a} \cdot \rho C_p \qquad (6')$$

$$LE = \frac{e(Z_o) - e(Z_T)}{r_a} \cdot \frac{\rho C_p}{\gamma} \qquad (7')$$

In order to evaluate H and LE, the temperature $T(Z_o)$ and the vapour pressure $e(Z_o)$ have to be estimated at the surface. Monteith introduced another resistance, the so called stomatal resistance r_{st}, given by

$$LE = \frac{e_s(T(Z_o)) - e(Z_o)}{r_{st}} \cdot \frac{\rho C_p}{\gamma} \qquad (7')$$

where $e_s(T(Z_o))$ is the saturated vapour pressure at the temperature $T(Z_o)$.

Evaporation from the surface is assumed to be mainly via the myriads of intercellular spaces - the stomata, the microscopic openings of the surface

of the leaves. The water vapour pressure inside the stomata is the saturated value at the leaf temperature, which can be assumed to be $T(Z_o)$ (Szeics and Long, 1969). The evaporation then depends on the state of the stomata (whether they are open or closed) and the difference between the saturated vapour pressure inside the stomata and the water vapour pressure outside. r_{st} does not therefore depend in any direct sense on atmospheric turbulence. r_{st} will be studied in more detail later on the basis of actual data.

Let $\Delta = \partial e_s(T)/\partial T$, and

$$\bar{\Delta} = \frac{\Delta(T(Z_o)) + \Delta(T(Z_T))}{2} \qquad (19)$$

Then

$$e_s(T(Z_o)) \approx e_s(T(Z_T)) + \bar{\Delta}(T(Z_o) - T(Z_T))$$

$$\sim e_s(T(Z_T)) + \bar{\Delta}.\ r_a.H/\rho Cp \qquad (20)$$

Combining (20) with equation (1), and using (7) and (18), gives Monteith's main result:

$$LE = \frac{\bar{\Delta}.\ r_a/\gamma + r_i}{r_{st} + (1 + \bar{\Delta}/\gamma)r_a} \cdot (R_n - G) \qquad (21)$$

where

$$r_i = [e_s(T(Z_T)) - e(Z_T)] \cdot \frac{\rho Cp}{\gamma} \cdot \frac{1}{R_n - G} \qquad (22)$$

r_i is called the 'climatological resistance' and is related to the humidity of the surface layer. The complementary equation to (21) gives the required heat flux,

$$H = \frac{r_a + r_{st} - r_i}{(1+\bar{\Delta}/\gamma)\, r_a + r_{st}} (R_n - G) \qquad (23)$$

4. The stomatal Resistance r_{st}

As mentioned above, the stomatal resistance r_{st} depends on the surface conditions, namely the physiological properties of the vegetation and the micro-meteorological state in the vegetated surface; the latter is mainly defined by the water content of the soil and the temperature of the surface layer.

If the surface energy balance data, i.e. R_n, G and LE or H, have been measured directly, then (22) or (23) can be used in reverse to estimate the value of r_{st}. (The estimation of r_a, r_i and $\bar{\Delta}$ will be presented later). Fig 15 shows the daily variation of r_{st} at Cardington, for six months, Apr-Sep, 1976, obtained in this way. The mean value of r_{st} for the four-hour period around midday (10-13 GMT) is considered. The daily mean temperature ((MAX+MIN)/2) and rain records are shown at the top of the same figure. It can be seen that:

(a) In the two hot/dry spells of the year, in late June to early July and in August, the stomatal resistance became much higher than that in the other periods of the year. This is because of the abnormal dryness and the consequent change in the surface state. The stomatal openings become very

small when insufficient water is available to the plants from the soil.

(b) Rainfall is the main factor affecting the variations of r_{st}. After any appreciable rainfall (daily rain $\geq$ 1mm) r_{st} drops rapidly to its normal low value (round 50). Afterwards, r_{st} increases day by day, more quickly when the temperature is higher (as in late June).

By late August the grass and soil had become extremely dry, resulting in the rather slow recovery of r_{st} in September when sporadic rains were experienced. This situation lasted until late September. From October to March of the next year the stomatal resistance kept to a low value (less than 200), the variation being similar to that in April 1976, which is shown in the figure.

Based on this analysis the following model can be used for estimating r_{st}:

Spring (Mar-May)

$$r_{st} = \begin{cases} 40\ d^{1/2} & (T \leq 10°C) \\ 50\ d & (T > 10°C) \end{cases}$$

Summer and early Autumn (Jun-Sep)

i) Green grass

$$r_{st} = \begin{cases} 50 + 50\ d & (T < 15°C) \\ 50 + 100\ d & (T \geq 15°C) \end{cases}$$

ii) dry grass

$$r_{st} = \begin{cases} 500 + 50d & (T < 15°C) \\ 500 + 100d & (T \geq 15°C) \end{cases}$$

(24)

Autumn and Winter (Oct-Feb)

$$r_{st} = 50.d^{1/2}$$

where d is the number of days after an appreciable rainfall ($\geq$ 1mm). If the daily rainfall is less than 1 mm, then r_{st} keeps the value of the previous day. T is the mean temperature of that day.

This is rather a rough model, but it is easy to use. Table 3 gives an example of the use of this model in estimating the daily r_{st} for the period of Apr-Jun, 1976, Cardington. The daily records of rainfall, mean temperature and the mean actual r_{st} of 10-13 hours are presented as well. The agreement between 'actual' and model r_{st} is mostly good. The large differences between the two arise on some days, e.g. 17-19, May, because the 'actual' r_{st} is a midday mean value, but the rainfall occurred later in the day.

The analysis above is only for around midday, probably suitable for 9-16 hrs local time. The variation of r_{st} with time of day is shown in Fig 16. The two solid lines in Fig 16 represent a two-month (May-June) mean and a four-month (May-Aug) mean respectively. The trends are very similar. The value of r_{st} in the early morning is much lower, particularly on a clear day with dew when $r_{st} \rightarrow 0$. The stomatal resistance increases with time till about 9 am, then keeps nearly the same value until about 5 pm. In the late afternoon, r_{st} sometimes becomes much larger for a few hours than the midday value. This may be a result of the reduced water supply after many hours of sunshine and strong evaporation. For the dry/hot period, 22-25, August, the hourly change of r_{st} is very large. But for spring, winter and some months in the Autumn, the stomatal resistance is rather

5. The aerodynamic resistance

The aerodynamic resistance r_a is governed by atmospheric turbulence. Because the latter is maintained by heat and momentum transfer, it is obvious that r_a depends on those quantities and can be expressed in terms of the known flux-profile relationships. Equation (17) gives an evaluation of r_a for neutral stratification. For the more general situation equations (13) and (14) (or (15)) should be used to evaluate r_a.

Based on the similarity function ϕ_m, ϕ_H given by Dyer and Hicks (1970), for the unstable case, we have:

$$\psi_m = \ln\left(\frac{X_2 - 1}{X_2 + 1} \cdot \frac{X_1 + 1}{X_1 - 1}\right) + 2\left(\tan^{-1} X_2 - \tan^{-1} X_1\right) \quad (28)$$

$$\psi_H = \ln\left(\frac{Y_2 - 1}{Y_2 + 1} \cdot \frac{Y_1 + 1}{Y_1 - 1}\right) \quad (29)$$

where $X_1 = (1 - 16\, Z_o/L)^{1/4}$, $X_2 = (1 - 16\, Z_u/L)^{1/4}$, $Y_1 = (1 - 16\, Z_o/L)^{1/2}$, $Y_2 = (1 - 16\, Z_T/L)^{1/2}$, $L = -(T/g) \cdot \rho C_p U_*^3/H$.

From (14) and (29)

$$r_a = \frac{1}{KU_*} \cdot \ln\left(\frac{Y_2 - 1}{Y_2 + 1} \cdot \frac{Y_1 + 1}{Y_1 - 1}\right) \quad (30)$$

Since U_*, H and L are at this stage unknown, an iteration method should be used for this evaluation. The procedure is as follows:

Step 1. Take the neutral case value of r_a (from (17)) as the first estimation. In this case

$$U_* = KU/\ln(Z_u/Z_o) \quad (31)$$

and H is estimated using (23), giving the first estimation of L.

Step 2. Substitute these estimations of U_* and L into (30), second estimations of r_a and H are obtained. A new U_* is derived by using

$$U_* = KU/\psi_m \qquad (32)$$

Step 3. Using the second estimates of H, U_* and L, return to step 2. Repeat this cycle until the successive values of r_a (or U_*, H, L) do not change by more than some specified required accuracy, say,

$$\left|\frac{I_N - I_{N+1}}{L_N}\right| < 0.01 \qquad (33)$$

In practice it appears that only very few steps (normally less than 3) are needed to achieve the required accuracy.

It is clear that at the end of the iteration quantities H and U_* are also obtained.

From (23)

$$\frac{\partial H}{\partial r_a} = H\left[\frac{1}{r_a + r_{st} - r_i} - \frac{1 + \bar{\Delta}/\gamma}{(1+\bar{\Delta}/\gamma).r_a + r_{st}}\right] \qquad (35)$$

or approximately

$$\frac{\Delta H}{H} = \left[\frac{r_a}{r_a + r_{st} - \gamma_i} - \frac{(1+\bar{\Delta}/\gamma).r_a}{(1+\bar{\Delta}/\gamma)\, r_a + r_{st}}\right] \frac{\Delta r_a}{r_a} \qquad (36)$$

Eq (36) can be used to evaluate the error of estimating H due to the error of estimating γ_a. Based on the data of two very unstable situations (May 9th, $r_a \approx 100$, $r_{st} \approx 200$, $r_i \approx 60$, $\bar{\Delta} \approx 2$; July 18th: $r_a \approx 100$, $r_{st} \approx 1000$, $r_i \approx 90$, $\bar{\Delta} \approx 2.6$).

$$\frac{\Delta H}{H} = -0.2\, \frac{\Delta r_a}{r_a} \qquad (37)$$

The estimation of H is thus not very sensitive to errors in the estimation of r_a. For some purposes the neutral case r_a, shown by (17), can be used in estimating an approximate value of H.

6. The other variables in Monteith formula

Here we present estimation formulae for the other variables appearing in the right side of the Monteith formula (23).

(a) R_n-G

The model for estimating R_n has been presented in section 2. The soil heat flux G at the surface depends very much on the type and state of the soil, the present and past history of R_n, and the state of vegetative cover. Fortunately it is a relatively small term, usually about 20% of R_n. The following equation can be used for the estimation:

$$R_n - G = (1.2 - 0.4 \frac{S}{S_m}) R_n \qquad (38)$$

where

$$S_m = \sin\phi \sin A + \cos\phi \cos A \qquad (39)$$

(b) γ_i

From (22)

$$r_i = \frac{\rho C_p}{(R_n - G)} [e_s(T) - e(z_T)] \qquad (40)$$

Here T is the measured temperature. The following approximate equations can be used in evaluating $e_s(T)$, ρCp, and :

$$e_s(T) = 6.11 + 0.4\ T + 0.025\ T^2 \qquad (41)$$

$$\rho Cp = 1305 - 4.3\ T \qquad (42)$$

$$\gamma = 0.646 + 0.0006T \qquad (43)$$

Given the dew point temperature T_d or the relative humidity h, one of the following equations can be used:

$$r_i = \frac{\rho Cp}{(R_n - G)} [e_s(T) - e_s(Td)] \qquad (44)$$

$$r_i = \frac{\rho Cp}{(R_n - G)} e_s(T)\ (1 - h/100) \qquad (45)$$

(c) $\bar{\Delta}$

As shown in (19), $\bar{\Delta}$ is taken as the average between Δ at temperature T and Δ at surface temperature $T(Z_o)$. $T(Z_o)$ can be evaluated by using of the flux-gradient relationship (6). But for the moment the following formula is suitable for practical use:

$$T(Z_o) = T + a.\ r_a\ .\ \frac{R_n - G}{\rho Cp} \qquad (46)$$

where

$$a = \begin{cases} 5.25\ .\ 10^{-3}\ r_{st} - 6.25\ .\ 10^{-6}\ .\ r_{st}^2 & (r_{st} < 400) \\ 1 & (r_{st} \geq 400) \end{cases} \qquad (47)$$

$\Delta = \partial e_s(T)/\partial T$ can be evaluated from (41), or more precisely

$$\Delta(T) = 0.45 + 0.02\ T + 0.0015\ T^2 \qquad (48)$$

Then,

$$\bar{\Delta} = 0.45 + 0.01\,(T+T_o) + 0.0008\,(T^2 + T_o^2) \qquad (49)$$

where $T_o = T(Z_o)$.

7. Discussion

A method has been presented for estimating heat flux (and momentum flux) based on routine data reported by standard meteorological stations. The model for estimating net radiation has been proved by several independent experiments. Combining with the simple model (24) for evaluating r_{st} (not considering the hourly variation of r_{st} in the morning or directly after rain), the sensible heat flux can be calculated by (23). Fig 17 shows a comparison of the sensible heat flux calculated by this method with the observed values, for the Cardington data, 1976, where the observed values of sensible heat flux were derived from the measurements of net radiation (by Kew-type radiometer), soil heat flux (by standard heat-flux-plates) and latent heat flux (by lysimeter), using the energy balance equation (1). This comparison shows reasonable results: the correlation is 0.84, and the standard error 32 W/m^2. Fig 18 gives a comparison for the Cardington data, 1983, in which the 'observed' sensible heat flux was derived from wind and temperature profile measurements of a 16 m mast. A finer model of evaluating r_{st}, i.e. considering the hourly variations of r_{st} in the morning and after rain, has been used. Fig 19 shows a comparison of the friction velocities, in which the U_* calculated by the iteration method given in section 5 was compared with the values derived from the wind profile data. The agreement is satisfactory.

We can conclude that the resistance method is a practical and useful method in estimating the fluxes, particularly as profile measurements and other direct measurements of the fluxes are not usually available. It is

clear from the analysis above that the resistance method is suitable for locations where the ground is covered with dense vegetation, such as short grass. For stations with rather bare ground the resistance method must be used with care.

Acknowledgement

I am grateful to Dr F B Smith for his valuable guidance in this research.

Appendix 1

Dr F B Smith's model of estimating r_{st}:

Let W be the present weather code ($W \geq 2$ implies precipitation, $W = 0,1$ implies no precipitation) and R an indicator of soil moisture content,

$R = 1$ soil wet;

$R = 2$ soil contains adequate moisture;

$R = 3$ soil dry

which is obtained from M (the state of ground code),

$M = 0$ surface dry

$M = 1$ surface moist

$M = 2$ surface wet . $H = 0$

$M \geq 3$ snow or ice covered

Then if d is the number of days after the last rain,

$d \leq 5$ days $M = 0$. $R = 2$

$M = 1$. $R = 1$

$5 < d < 10$ $M = 0, 1$. $R = 2$

$d \geq 10$ $M = 0$. $R = 3$

$M = 1$. $R = 2$

r_{st} can be estimated as follows:

Oct - March

$r_{st} = 80$ if $W = 0,1$

$r_{st} = 0$ if $W \geq 2$

April - Sept

$r_{st} = 0$ if $W \geq 2$

$r_{st} = 50$ if $W = 0,1$ and $R = 1,2$

$r_{st}(n) = r_{st}(n-1) + 10 (T_{max} - 10)$ if $W = 0,1$ and $R = 3$ and $T_{max} > 10$

References

Clarke, R.H. et al, 1971, 'The Wangara Experiment: Boundary Layer Data', Div. of Met. Phys. Technical Paper No 19, CSIRO, Australia.

Dyer, A. J. and B. B. Hicks, 1970, 'Flux-gradient relationships in the constant flux layer', Quart. J.R. Met. Soc., 96, 715-721.

Garratt, J.R. et al, 1979, 'The International Turbulence Comparison Experiment (Australia, 1976) - Micrometeorological support Data', Div. of Met. Phys. Technical Paper No 37, CSIRO, Australia.

Lumb, F.E., 1964, 'The influence of cloud on hourly amounts of Total Solar Radiation at the sea surface', Quart. J.R. Met. Soc., 90, 43-56.

Monteith, J. L., 1965, 'Evaporation and Environment'. In 'The state and movement of water in living organisms'. 19th symp. Soc. Exp. Biol., 205-235.

Nielsen, L.B. et al, 1981, 'Net Incoming Radiation Estimated from Hourly Global Radiation and/or Cloud observations'. J. Climatology, 1, 255-272.

Smith, F.B. and R. D. Hunt, 1978, 'Estimation of sensible heat flux over Grassland'. TDN No 91. Meteorological Office, U.K.

Szeicz, G. and I.F. Long, 1969, 'Surface resistance of Crop Canopies' Wat. Resour. Res., 5, 622-633.

LIST OF FIGURES

Fig 1. The hourly variation of Rn on a normal 'partly cloudy' day, 10 May 1983, Cardington. The curve was drawn based on the 10 min. average data, of which the reading was taken every 10 sec. The hourly cloud reports presented on the top, total amounts are shown in the circles.

● hourly mean value

o Calculated value by our model (Eq (2), Table 1)

correlation = 0.94.

Fig 2. The scatter of Rn under two extreme cloud states.

● clear sky (no cloud, a few hours of total amount ≤ 2)

o overcast (total amount ≥ 7, excluding C_H)

(Based on Cardington data, May-Aug, 1976; 20 clear days, 15 cloudy days).

Fig 3. The scatter of R_n with respect to solar elevation S under two cloud conditions. (● condition I, o condition II).

curve I : $R_n = -172.1S^3 + 742.2S^2 + 102.5S - 45.0$

curve II: $R_n = 99.6S^3 + 155.9\,S^2 + 41.6S + 6.2$

(Based on Cardington data, 50 days in Apr-Aug, 1976. 32 days of cloud condition I (15 clear days), 18 days of cloud condition II).

Fig 4. Comparison of observed net radiation (R_{no}) with calculated (R_{nc}) by the model. The data set is same as in Fig 3. The statistical comparison of R_{no} and R_{nc}:

	Mean	Standard Div (σ_n)	correlation (Γ)	Standard error (SE)
R_{no}	202	152	0.95	48
R_{nc}	195	140		

Fig 5. Same as Fig 3, but based on the 1982 experiment, 2-20 June, Cardington. Only 6 days can be used for this analysis.

Fig 6. Same as Fig 4, but for the same data as in Fig 5.

	Mean	σ_n	r	S.E.
R_{no}	181	169	0.93	62
R_{nc}	174	161		

Fig 7. Same as Fig 3, but based on the data of Cardington experiment, 20 Apr - 19 May 1983. The whole data, except rainy hours, had been used in analysis. There was no clear day in the experimental period.

Fig 8. Same as Fig 4, but for the same data as in Fig 7.

	Mean	σ_n	r	S.E.
R_{no}	186	148	0.92	60
R_{nc}	197	147		

Fig 9. Same as Fig 3, but based on the data of Kew, Apr-Aug 1978. 36 days had been used for analysis, including 21 days of cloud condition I (8 clear days), 15 days of cloud condition II.

Fig 10. Same as Fig 4, but for the same data as in Fig 9.

	Mean	σ_n	r	S.E
R_{no}	229	160	0.94	58
R_{nc}	213	150		

Fig 11. Same as Fig 3, but for Wangara data.

Here, curve I : $R_n = 400.0S^3 + 830.0\ S^2 + 269.05 - 45.8$

curve II: $R_n = 125.5S^3 + 159.0S^2 + 133.7S - 11.3$

Based on the whole Wangara data set, except rainy hours.

Fig 12. Same as Fig 3, but for the same data as in Fig 11.

	Mean	σ_n	r	S.E
R_{no}	172	125	0.92	50
R_{nc}	164	126		

Fig 13. Same as Fig 11, but for the ITCE experiment. Based mainly on 9 days data.

Fig 14. Same as Fig 3, but for the same data as in Fig 13.

	Mean	σ_n	r	S.E
R_{no}	305	197	0.94	72
R_{nc}	326	202		

Fig 15. Daily variation of r_{st}, Apr-Sep, 1976. Daily mean temperature and rain records are shown on the top. For appreciable rain the daily amount of rainfall are shown.

Fig 16. The hourly variation of r_{st} in day time. The average periods of the data are shown by each curve. Cardington data, 1976.

Fig 17. Comparison of modelling values (H_c) with observed values (H_o) of sensible heat flux, for the data of Apr-Jun, 1976, Cardington.

	Mean	σ_n	r	S.E.
H_O	114	59	0.84	32
H_C	113	50		

Fig 18. Same as Fig 17, but for Cardington data, Apr-May, 1983.

	Mean	σ_n	r	S.E
H_O	105	58	0.92	27
H_C	92	48		

Fig 19. A comparison for the friction velocity U*, based on the data of Cardington, 1983.

$U*_O$ - U * obtained by profile measurements.

$U*_C$ - U * calculated by resistance method.

	Mean	σ_{u*}	r	S.E.
$U*_O$	0.40	0.14	0.95	0.05
$U*_C$	0.38	0.12		

Date	Rainfall (mm)	T	r_{st} 'Actual'	r_{st} Model	Date	Rainfall (mm)	T	r_{st} 'Actual'	r_{st} Model
Apr 1	Tr	10	15	0	May 17	0.1	13	350	50
2	1.6	9	0	0	18	1.1	14	270	0
3		6	50	40	19	1.4	9	120	0
4	Tr	8	60	40	20	0.3	12	/	50
5	Tr	7	70	40	21		11	250	100
6	0.4	12	70	40	22		15	320	150
7	1.2	6	/	0	23		14	300	200
8	Tr	4	50	40	24	6.1	14	370	0
9		8	30	60	25	5.5	12	/	0
10		10	0	70	26	Tr	11	50	50
11		8	50	80	27		11	70	100
12	Tr	6	40	80	28	1.9	13	100	0
13	3.8	9	40	0	29	2.6	13	/	0
14	9.2	7	/	0	30		12	70	50
15		10	50	40	31	3.2	14	120	0
16	0.1	8	80	40	Jun 1	0.2	15	80	100
17		8	60	60	2	Tr	14	90	100
18	Tr	10	/	60	3		8	130	150
19		10	60	70	4	Tr	13	200	150
20		11	70	80	5	0.3	15	250	150
21		9	60	90	6		18	270	350
22		9	50	100	7		17	330	450
23	0.6	6	/	100	8		20	350	550
24	0.2	6	80	100	9		19	450	650
25	Tr	8	60	100	10		16	700	750
26	Tr	8	60	100	11	Tr	15	800	750
27	Tr	7	80	100	12	Tr	17	/	750
28		3	140	110	13		17	1100	850
29	Tr	4	/	110	14		18	1000	950
30	Tr	10	90	110	15	Tr	16	900	950
May 1	0.6	7	170	100	16	Tr	14	850	950
2	Tr	11	90	110	17	0.6	14	800	950
3	3.0	11	/	0	18	0.3	17	800	950
4	0.1	11	80	50	19	9.3	13	/	0
5	0.2	13	110	50	20		15	60	100
6		16	100	100	21		14	360	150
7	Tr	14	150	100	22		18	400	350
8		15	130	150	23		23	500	450
9	0.4	16	200	150	24		21	600	550
10		15	60	200	25		21	800	650
11	0.1	9	/	200	26		25	1000	750
12	2.0	11	/	0	27		25	1200	850
13	0.1	11	70	50	28		24	1400	950
14		9	350	100	29		21	1300	1050
15	2.6	10	/	0	30		21	1250	1150
16		11	200	50					

Table 3. The calculated value of r_{st} for Apr-Jun, 1976, Cardington, along with the data of rainfall, mean temperature (T) and the 'actual' value of r_{st} (the mean value for 10-13 GMT).

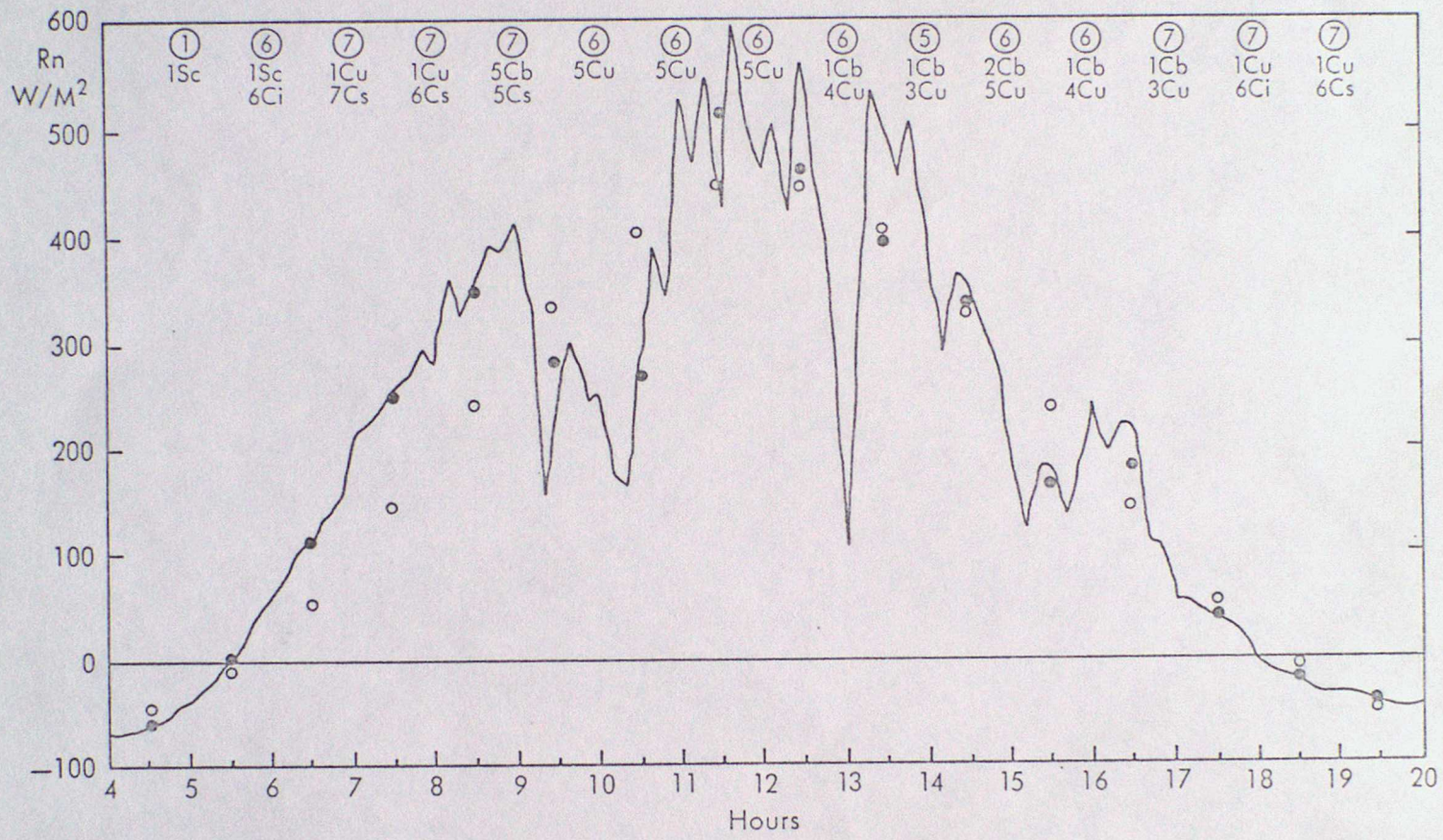
Rn
W/M²
600
500
400
300
200
100
0
−100
① 1Sc
⑥ 1Sc 6Ci
⑦ 1Cu 7Cs
⑦ 1Cu 6Cs
⑦ 5Cb 5Cs
⑥ 5Cu
⑥ 5Cu
⑥ 5Cu
⑥ 1Cb 4Cu
⑤ 1Cb 3Cu
⑥ 2Cb 5Cu
⑥ 1Cb 4Cu
⑦ 1Cb 3Cu
⑦ 1Cu 6Ci
⑦ 1Cu 6Cs
4 5 6 7 8 9 10 11 12 13 14 15 16 17 18 19 20
Hours

Fig 1

Fig 2

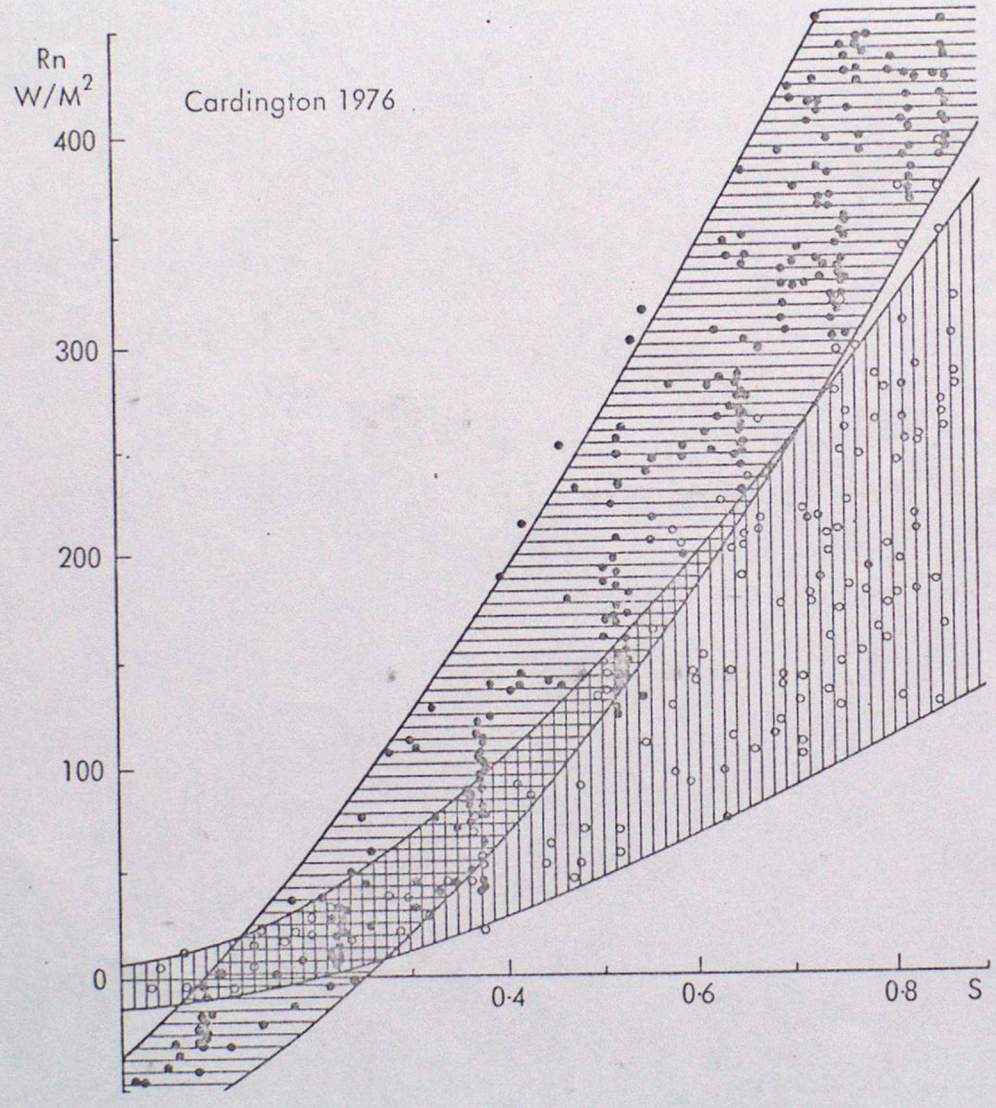

Fig 3

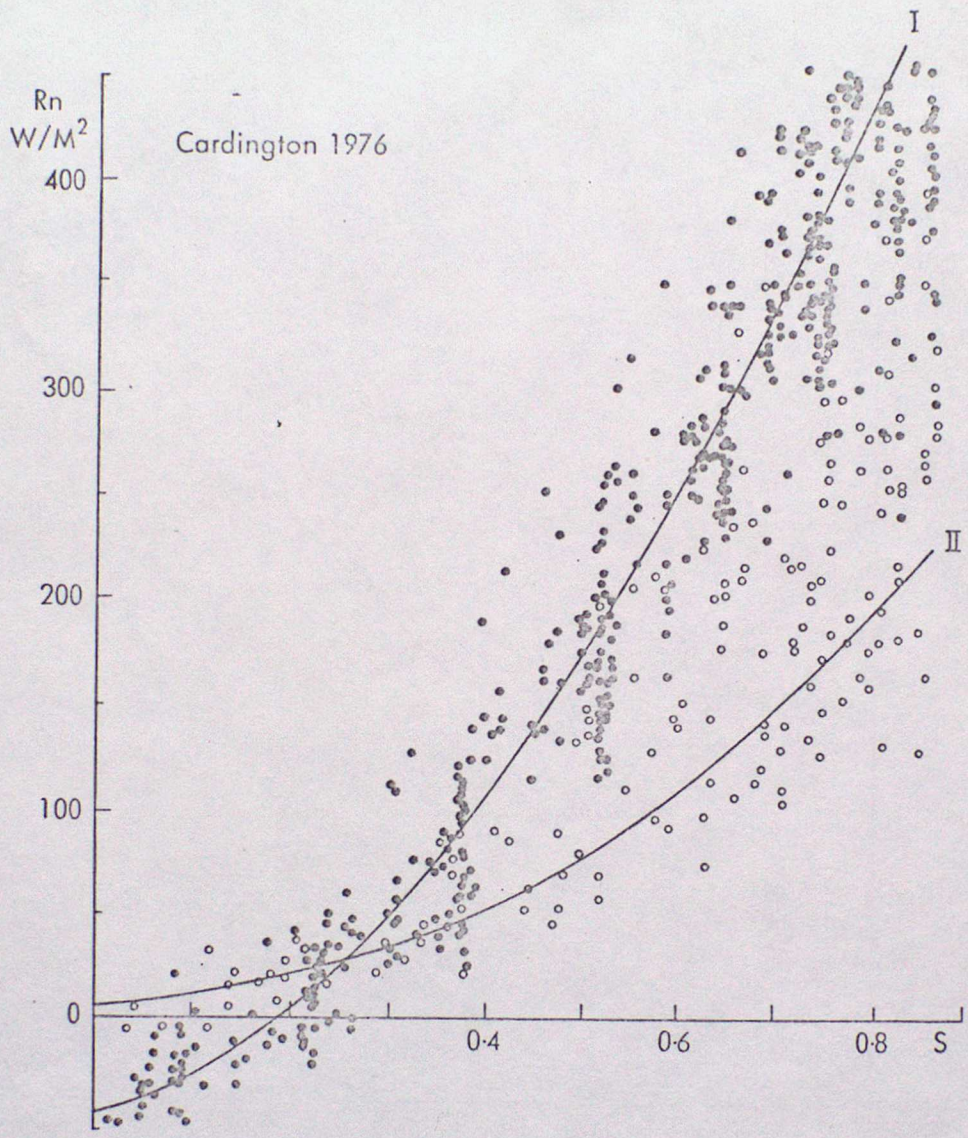

Fig 4

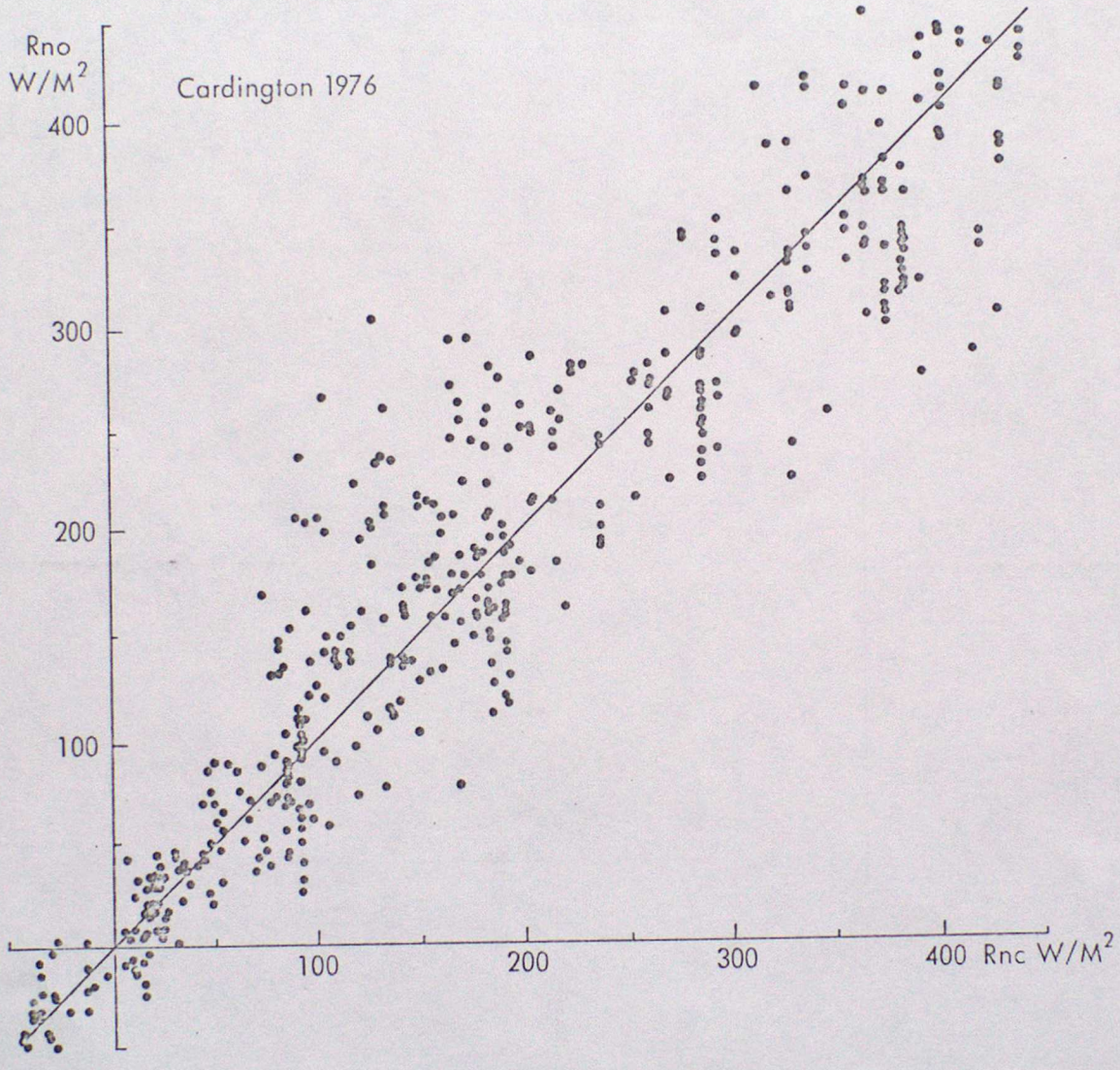
Rno
W/M²
Cardington 1976
400
300
200
100
100
200
300
400 Rnc W/M²

Fig 5

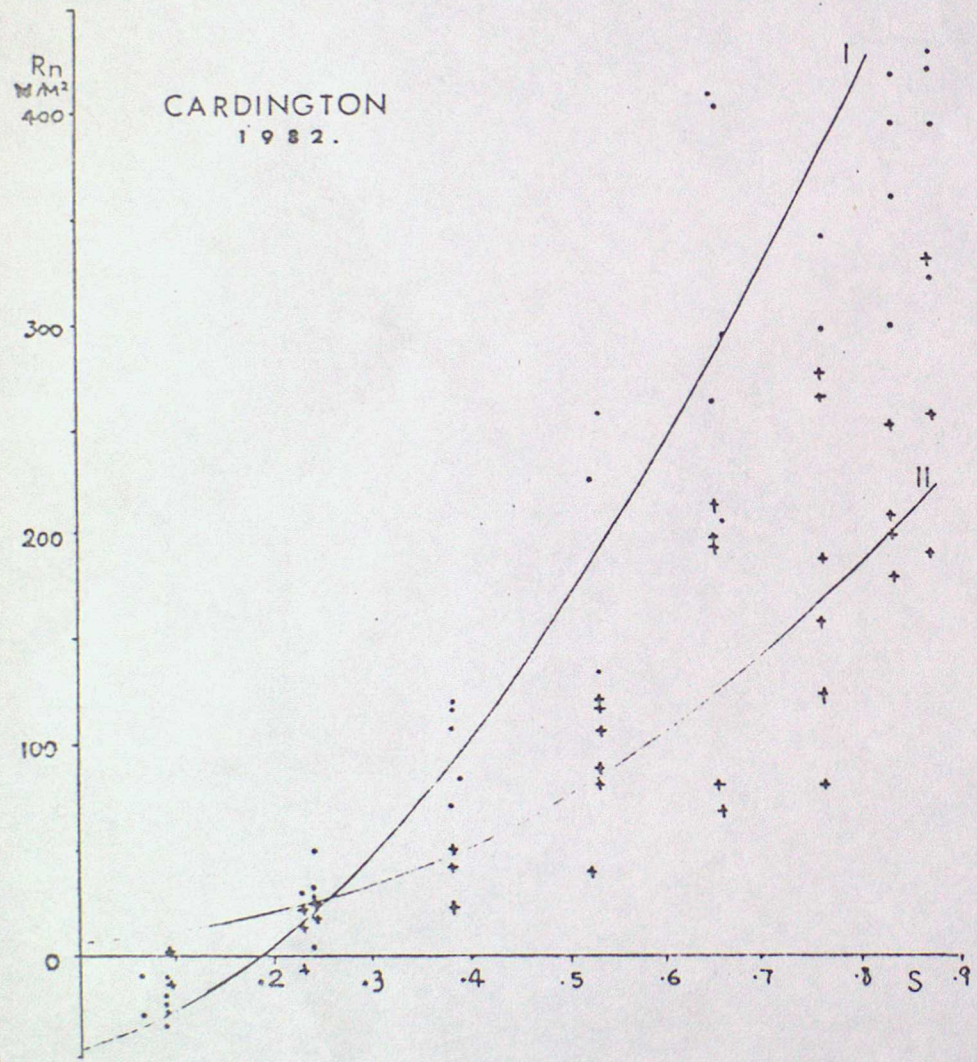
Rn
W/M²
400
300
200
100
0
CARDINGTON
1982.
I
II
·2
·3
·4
·5
·6
·7
·8
S
·9

Fig 6

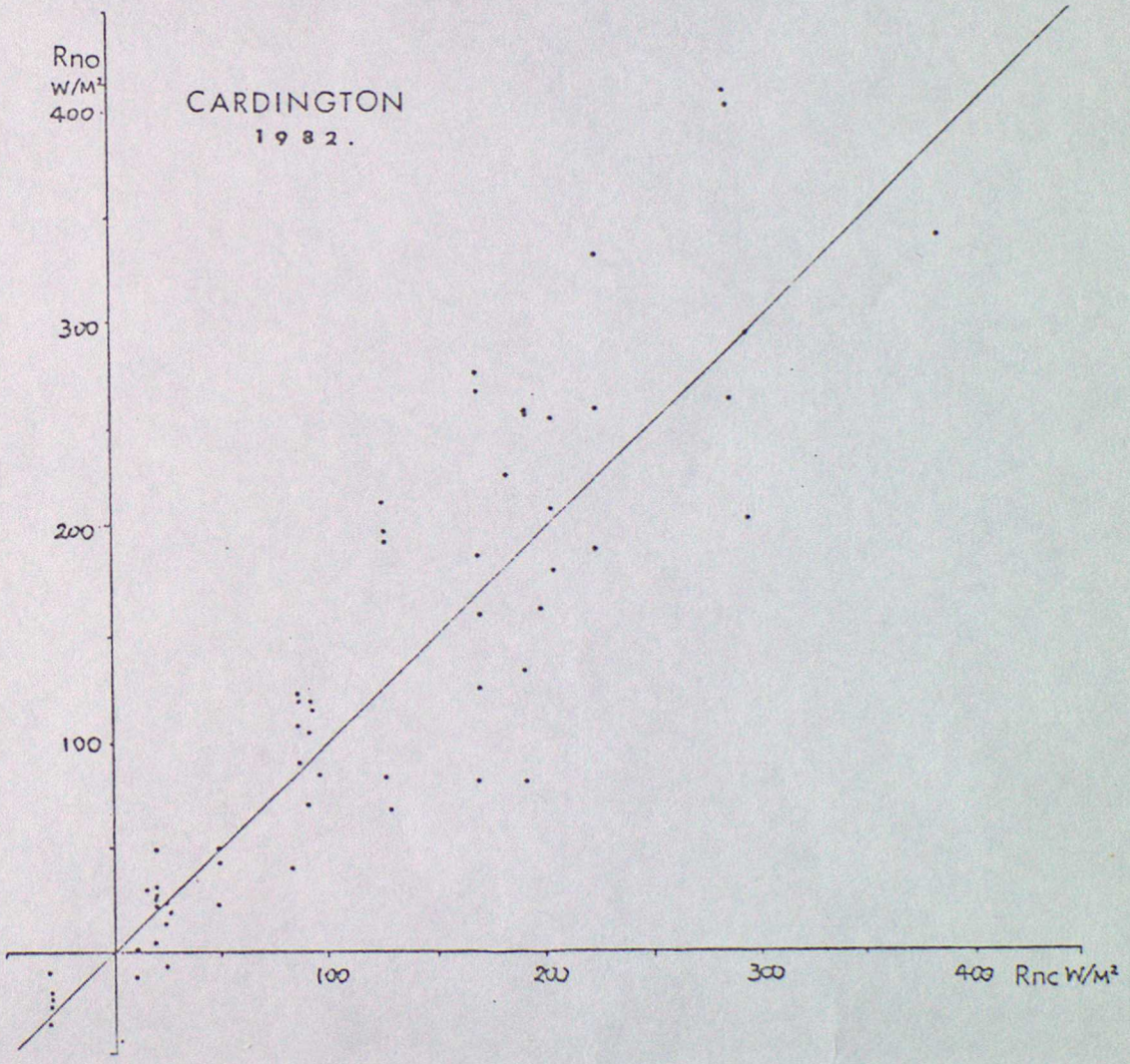
Rno
W/M²
400
300
200
100
CARDINGTON
1982.
100
200
300
400
Rnc W/M²

Fig 7

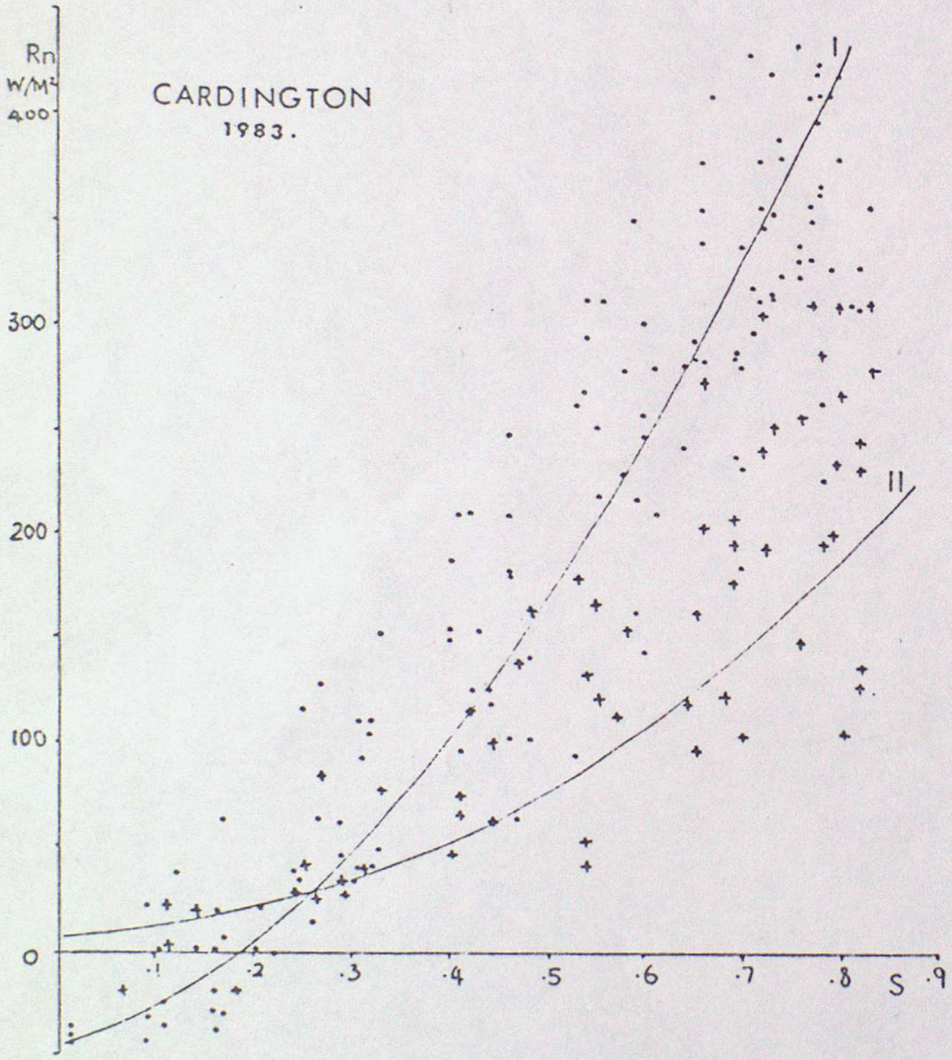
Rn
W/M²
400
300
200
100
0
CARDINGTON
1983.
I
II
·1
·2
·3
·4
·5
·6
·7
·8
S
·9

Fig 8

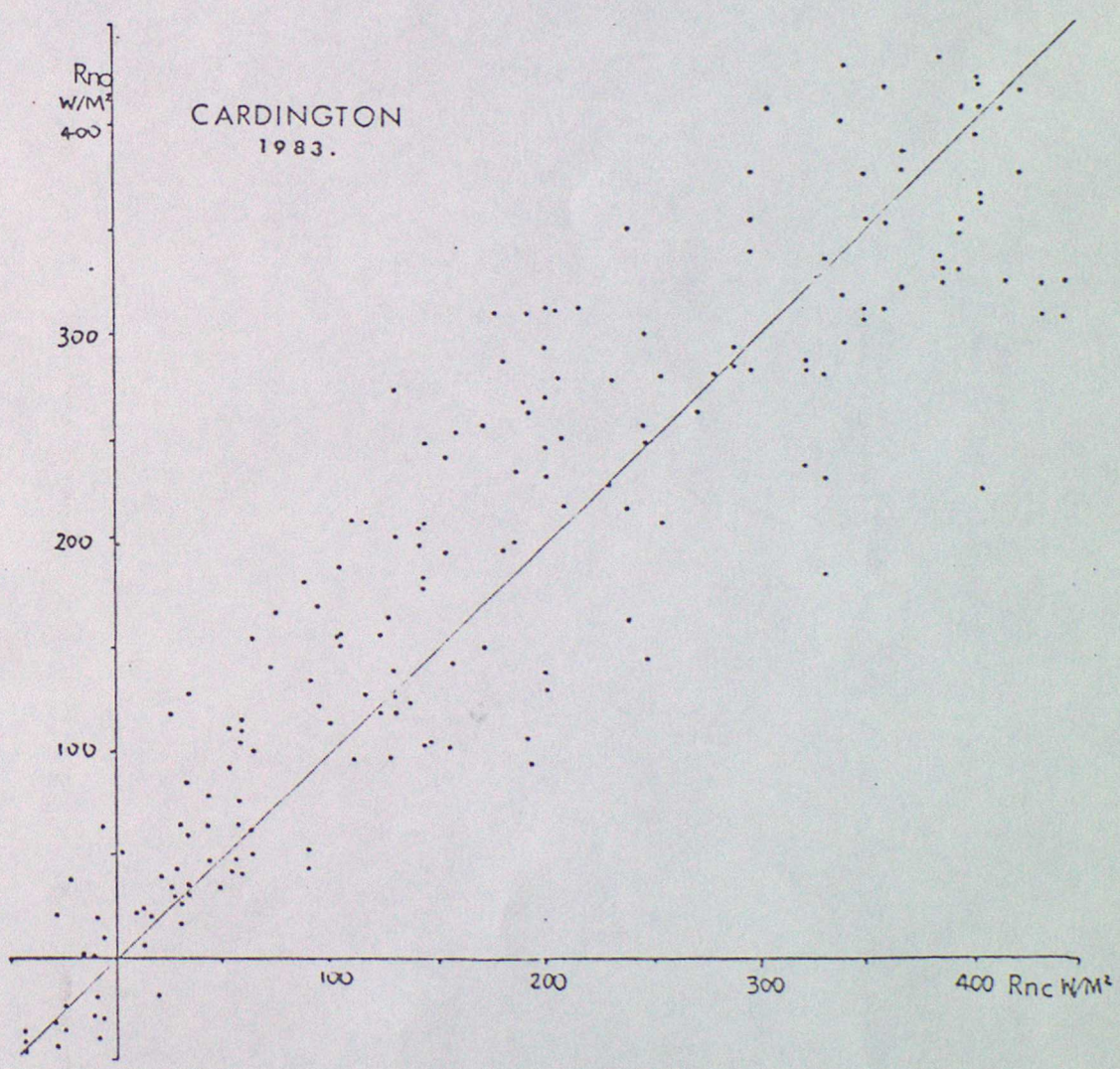
Rnc
W/M²
400
300
200
100
CARDINGTON
1983.
100
200
300
400 Rnc W/M²

Fig 9

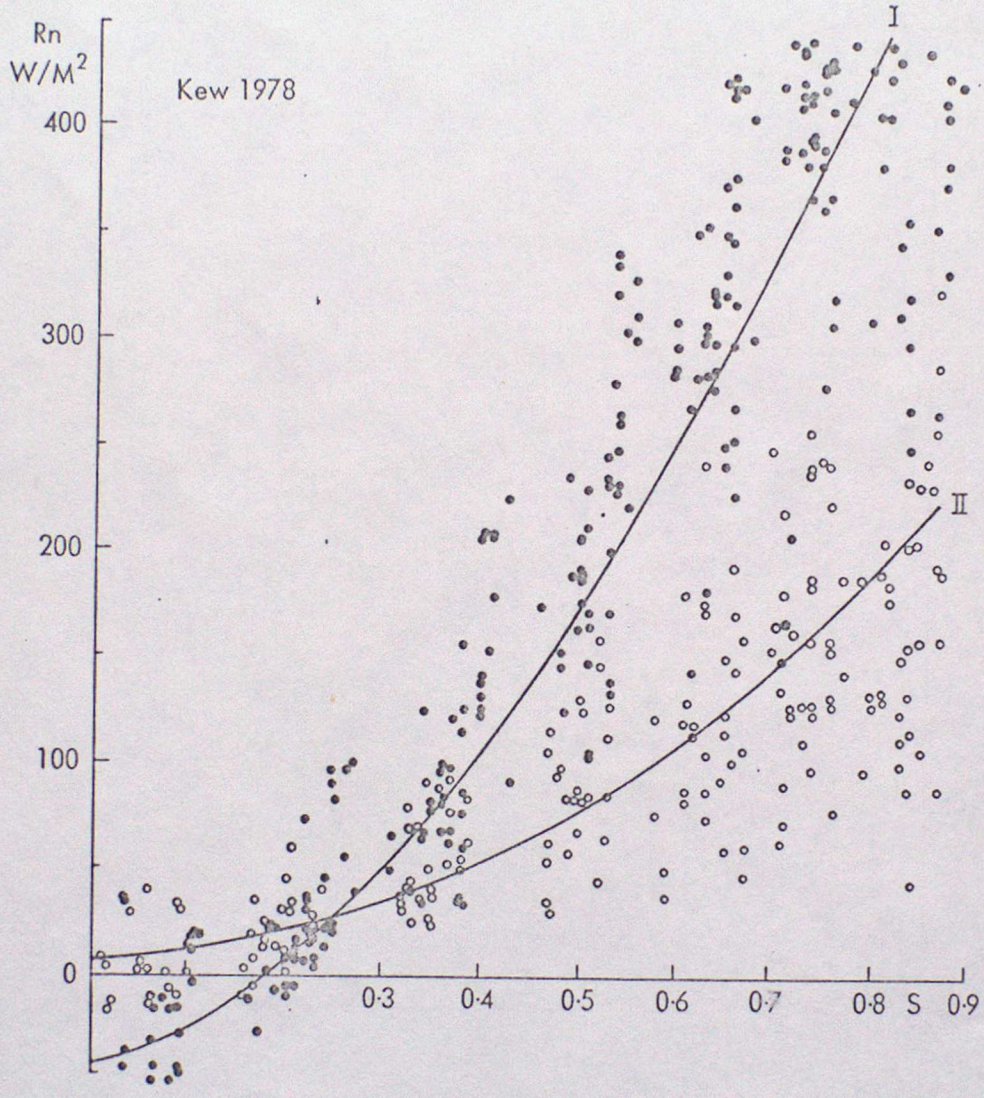

Fig 10

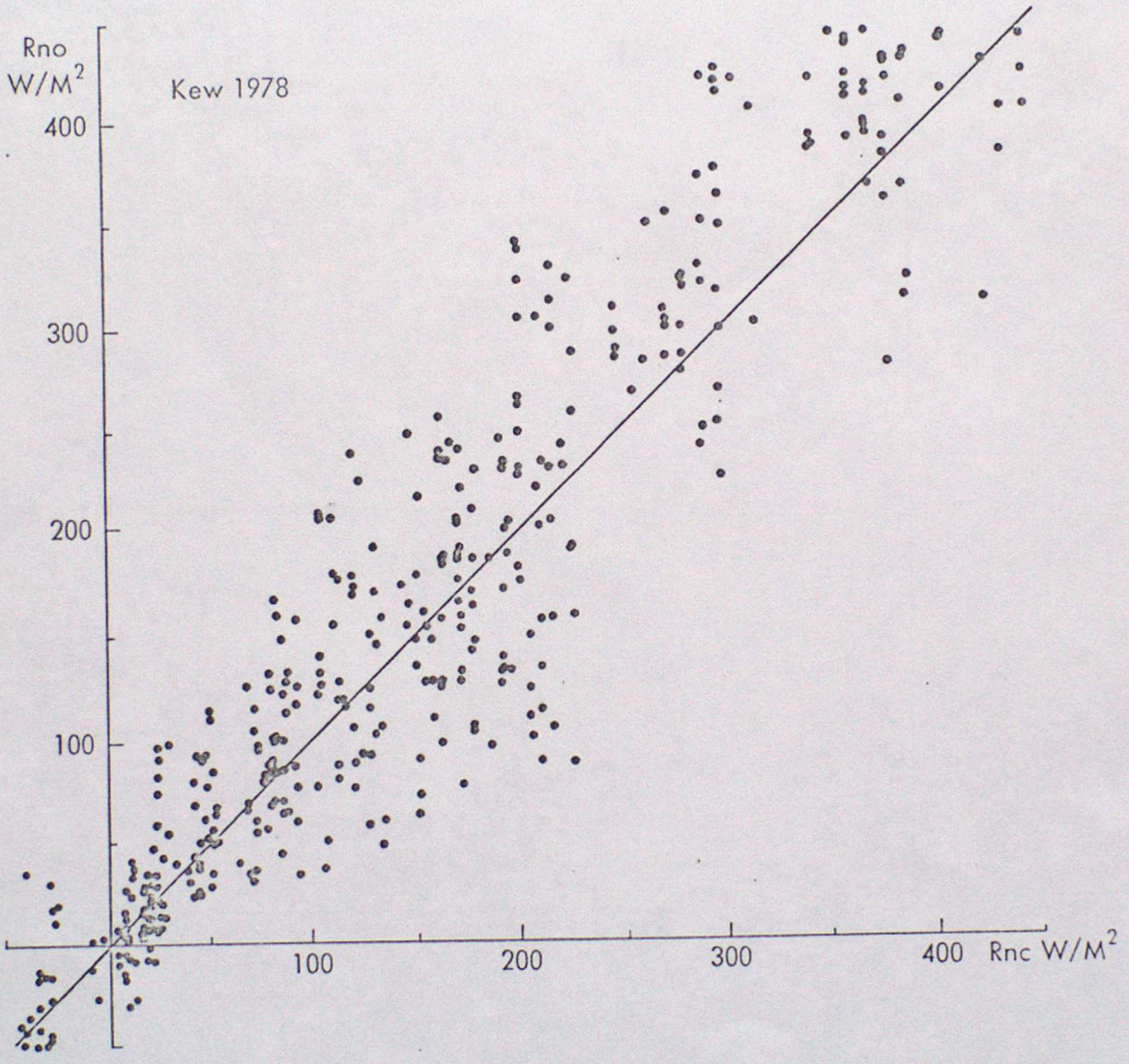

Fig 11

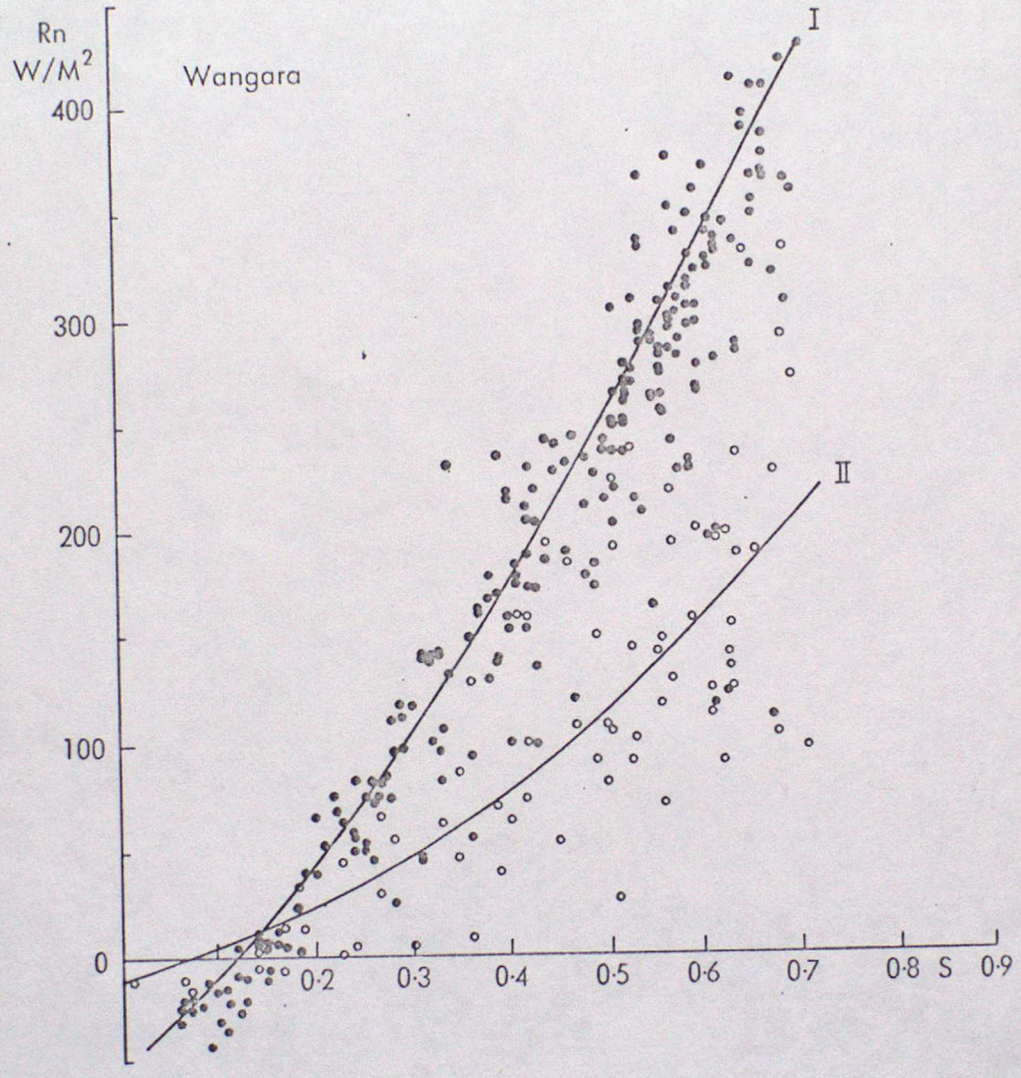

Fig 2.

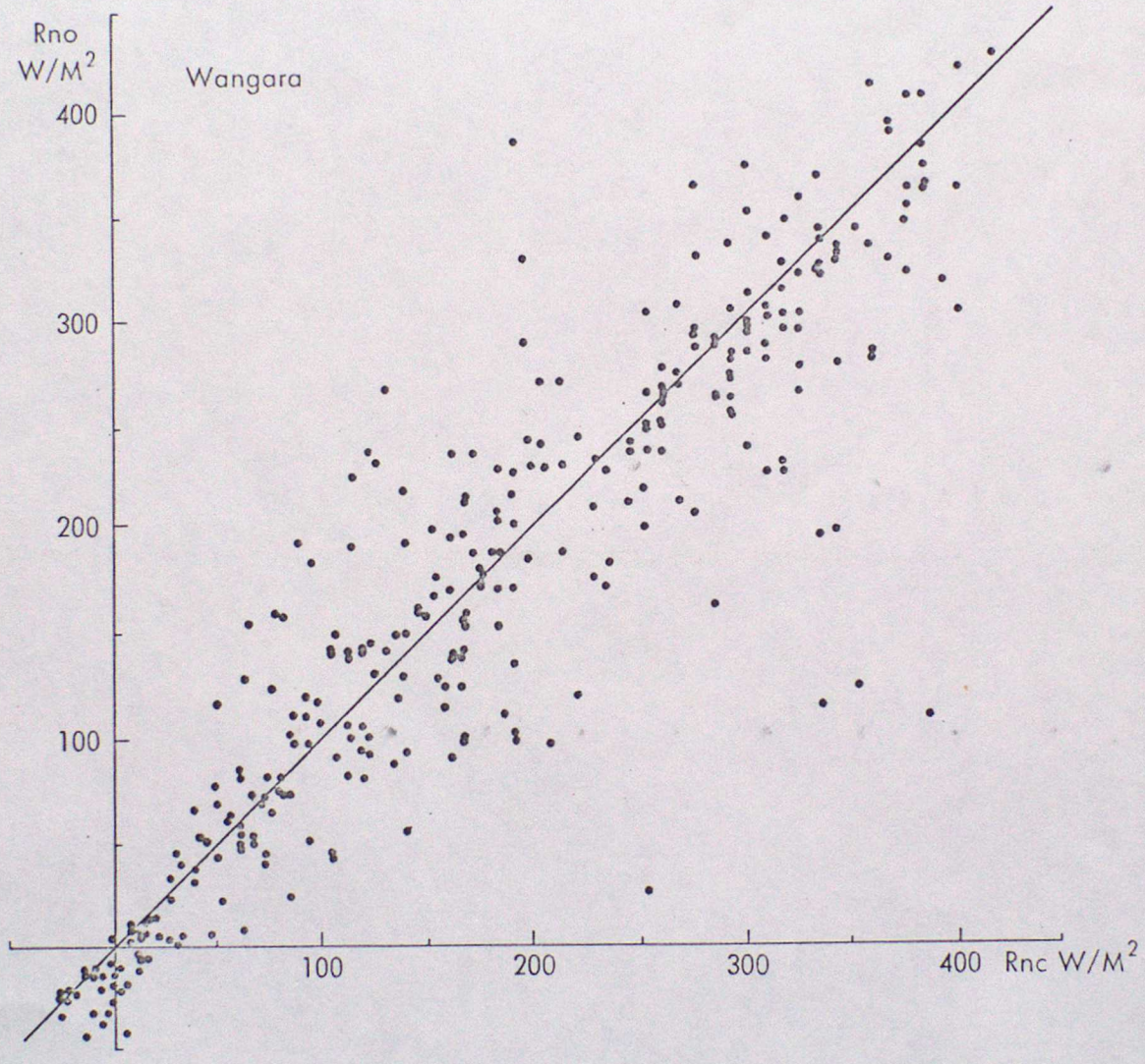

Fig 13

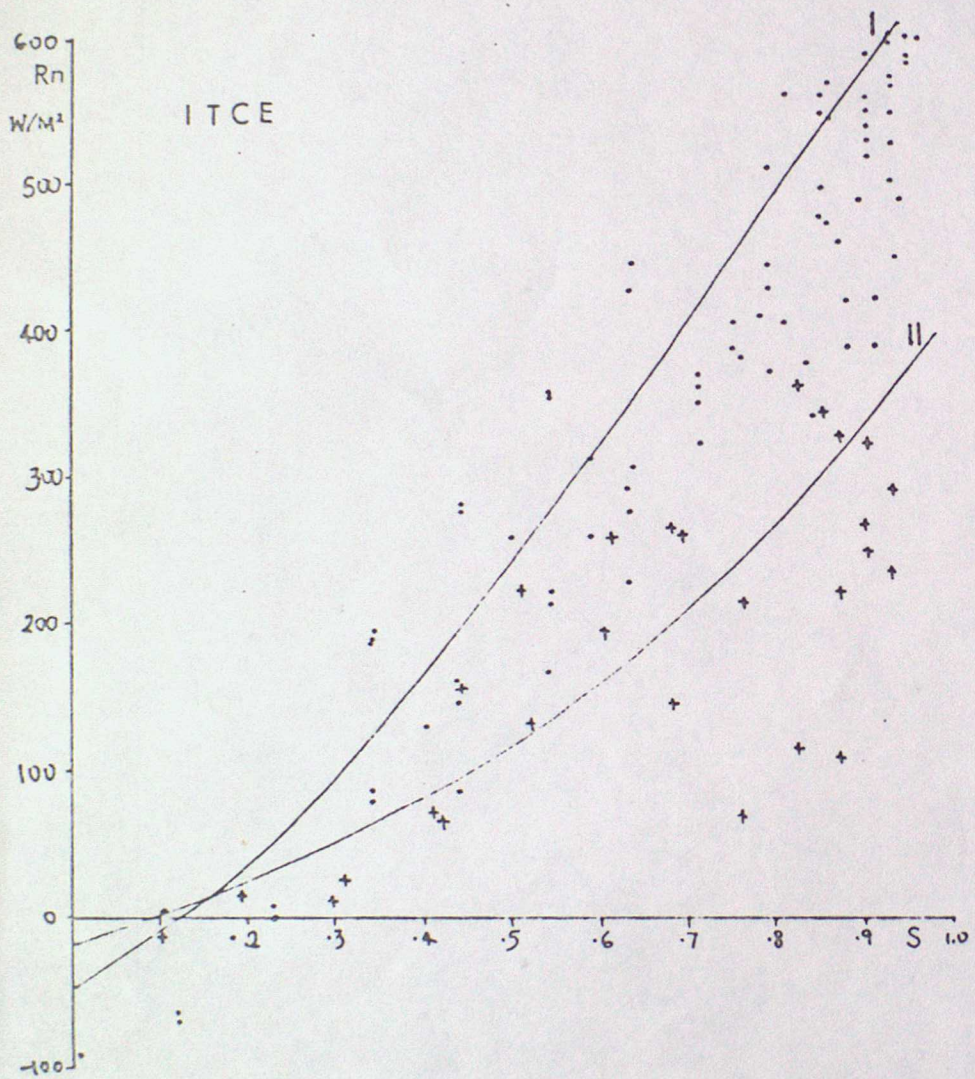
ITCE
Rn
W/M²
600
500
400
300
200
100
0
-100
I
II
·2
·3
·4
·5
·6
·7
·8
·9
S
1.0

Fig 14

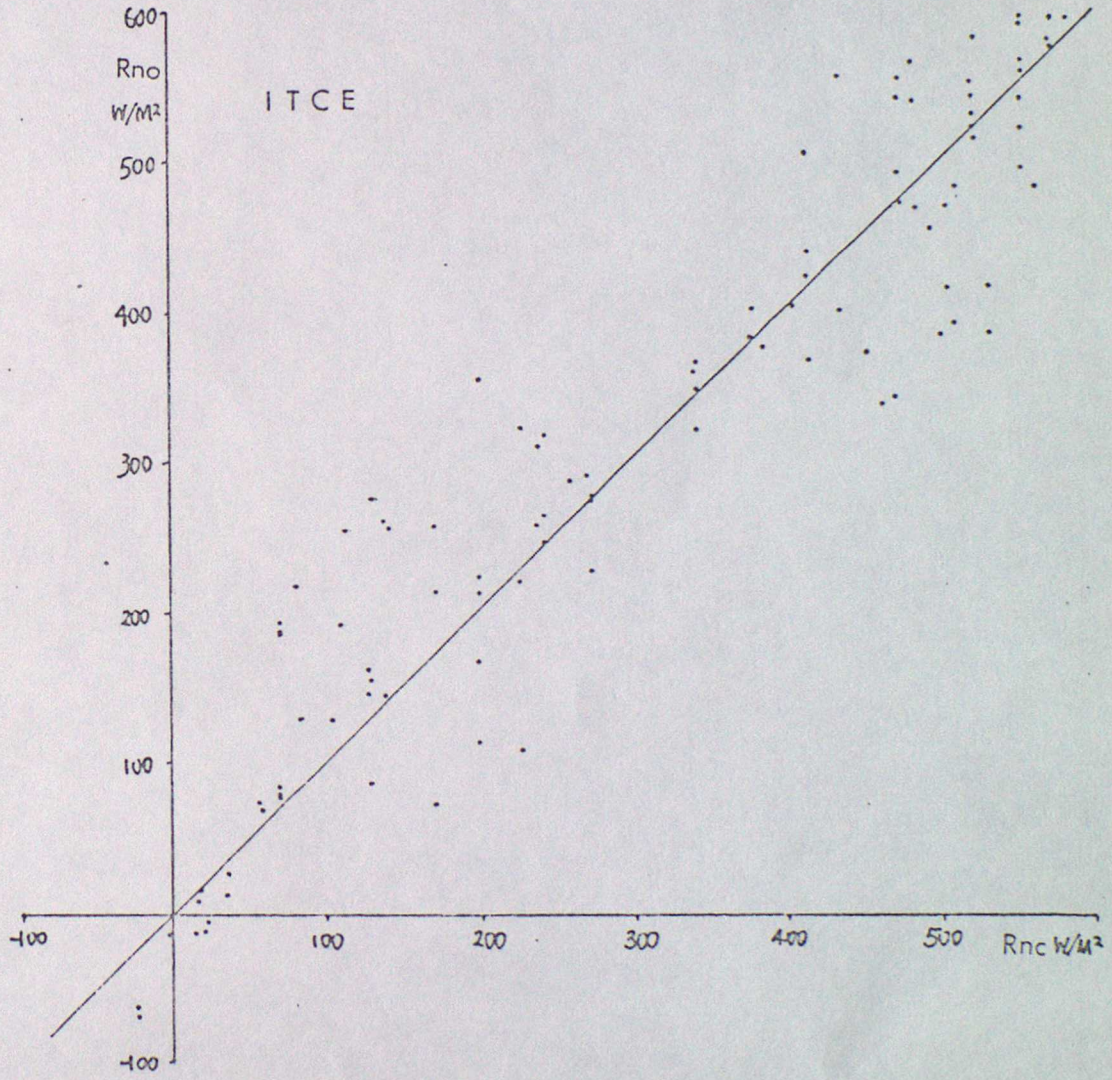
ITCE
Rno
W/M²
600
500
400
300
200
100
-100
100
200
300
400
500
Rnc W/M²

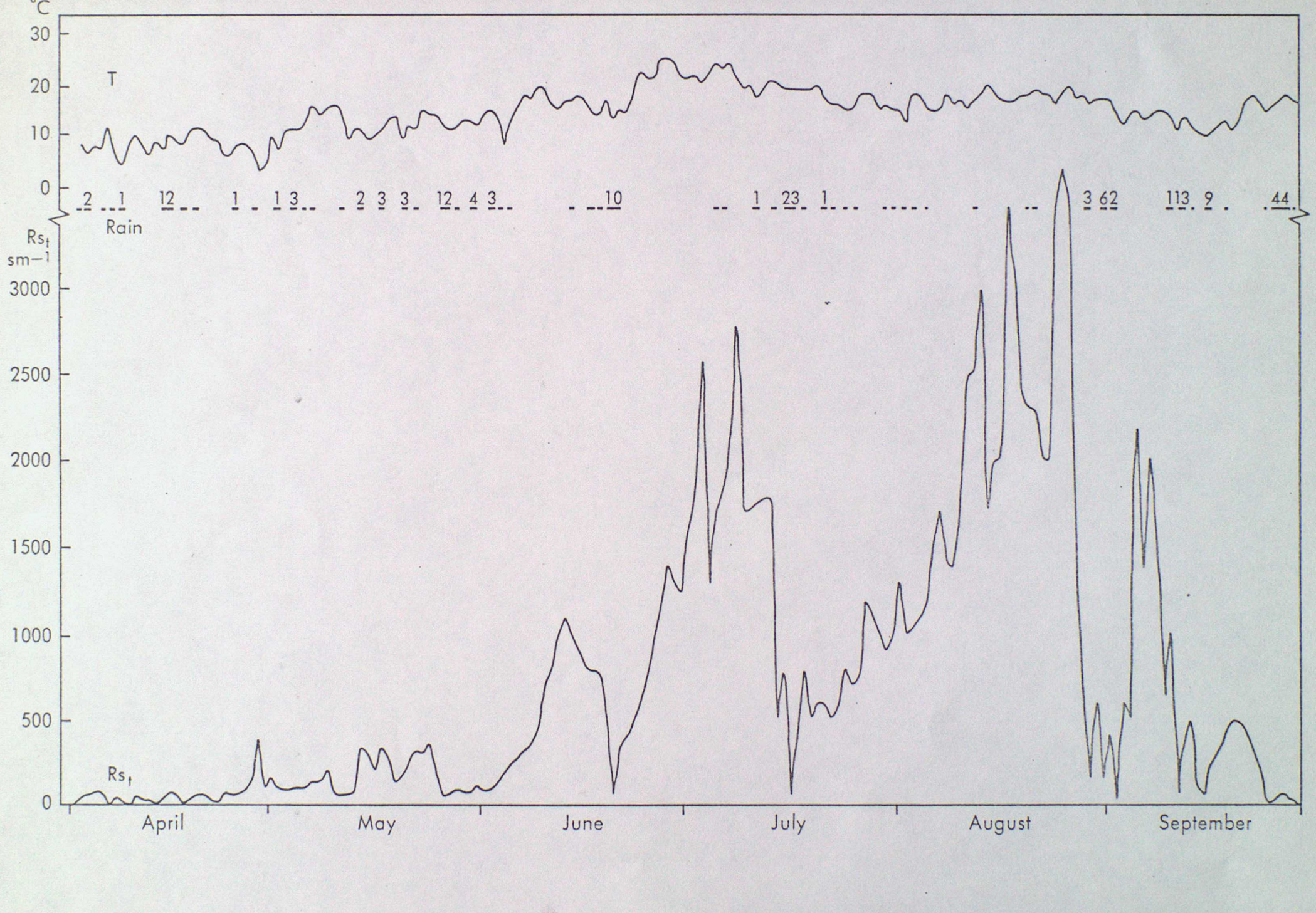
°C
30
20
10
0
T
2 1 12 1 1 3 2 3 3 12 4 3 10 1 23 1 3 62 113 9 44
Rain
Rs_t
sm⁻¹
3000
2500
2000
1500
1000
500
0
Rs_t
April
May
June
July
August
September

Fig 16

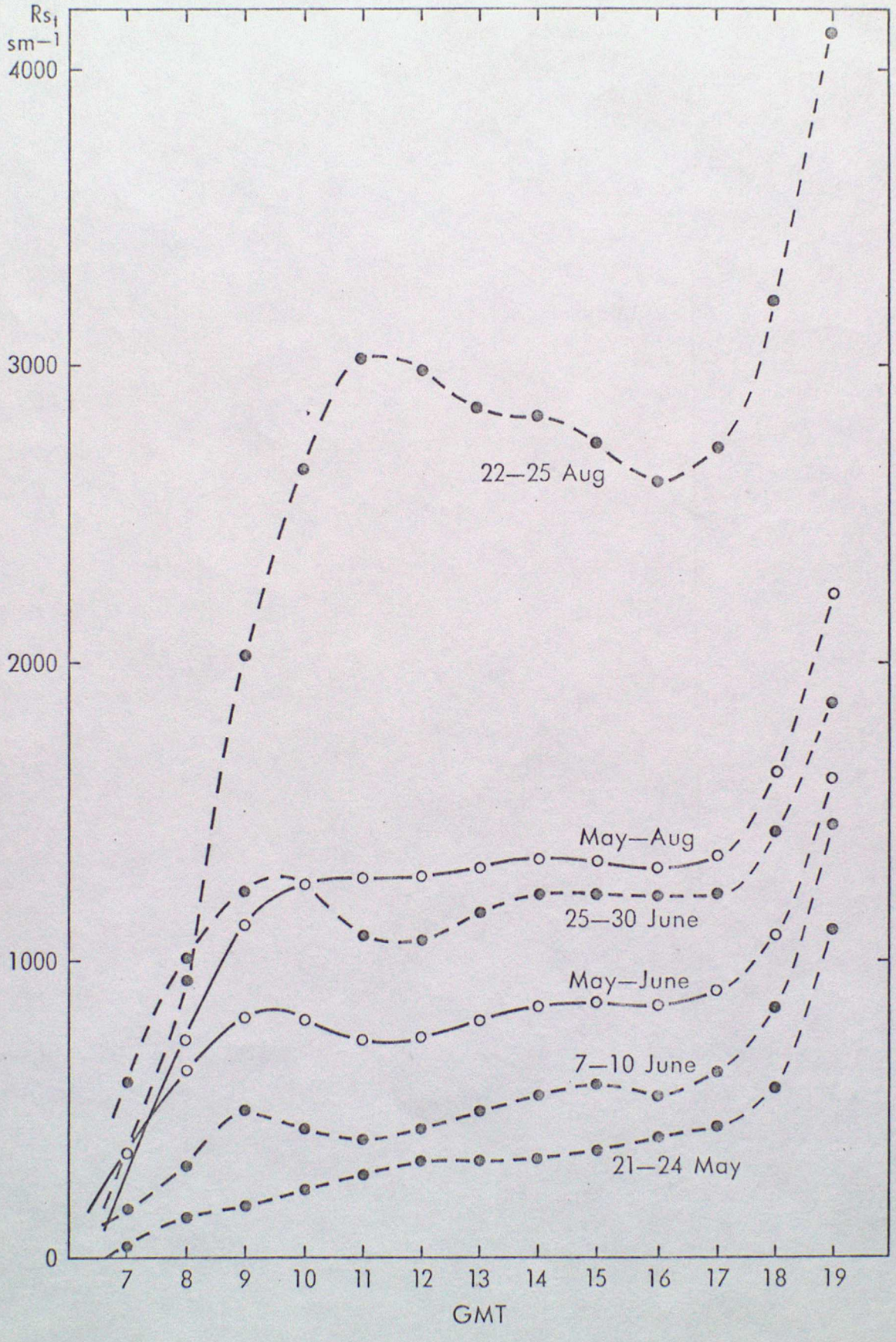
Rs_t
sm^{-1}
4000
3000
2000
1000
0
22—25 Aug
May—Aug
25—30 June
May—June
7—10 June
21—24 May
7
8
9
10
11
12
13
14
15
16
17
18
19
GMT

Fig 17

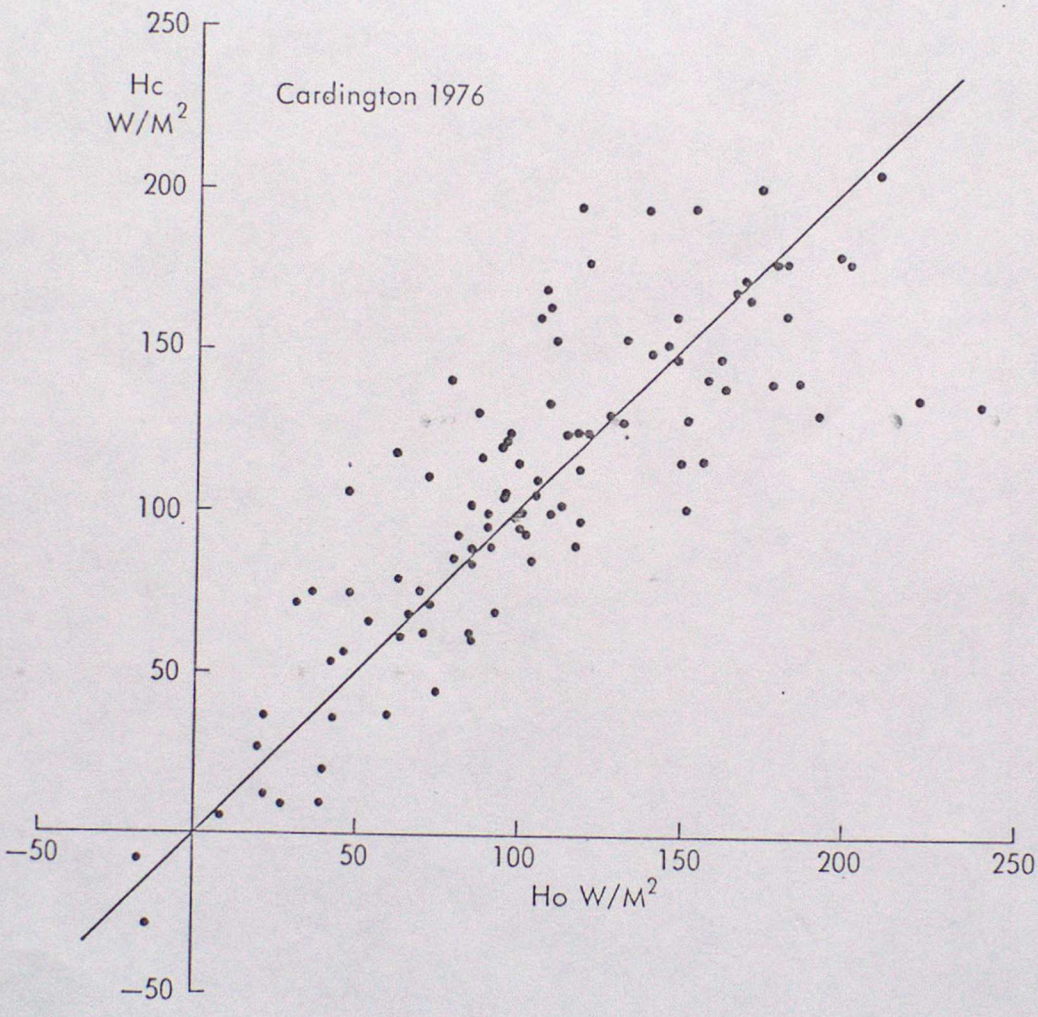
Cardington 1976
Hc W/M²
Ho W/M²
250
200
150
100
50
−50
−50
50
100
150
200
250

Fig 18

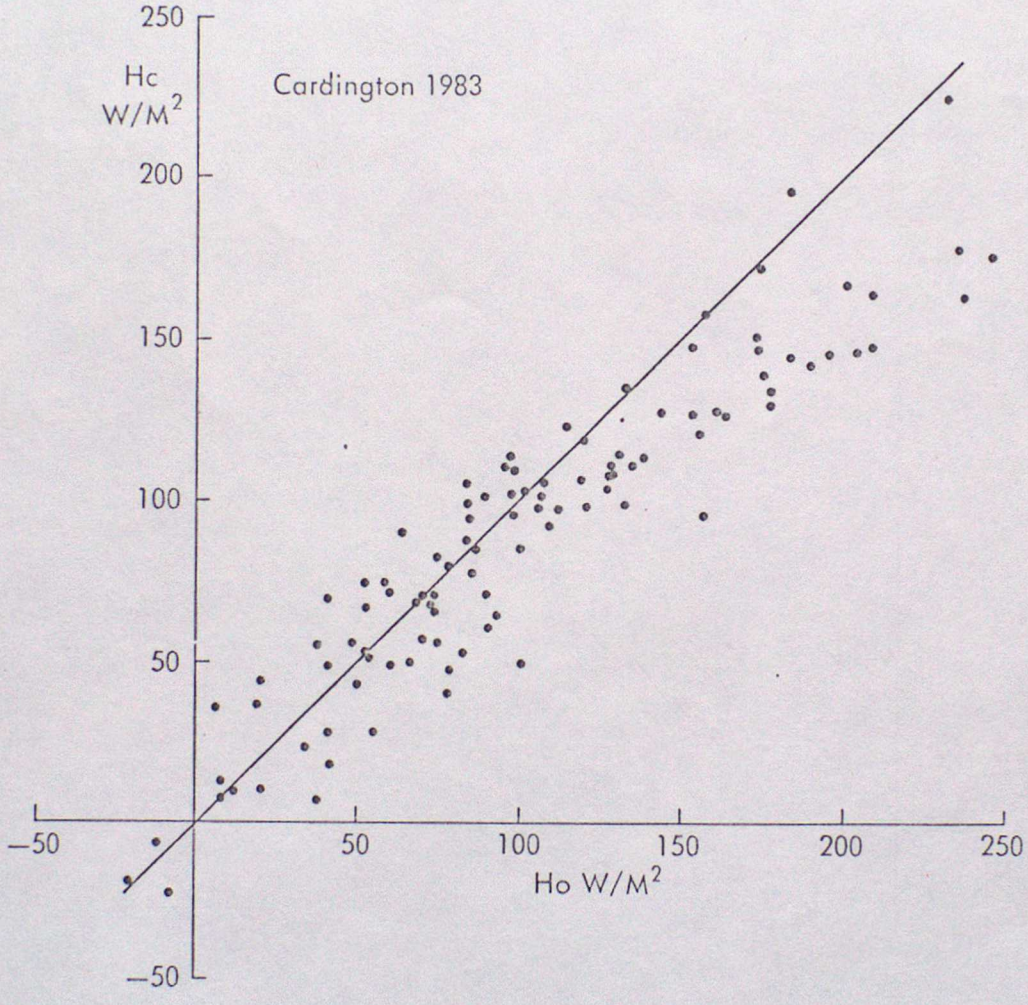
Cardington 1983
Hc
W/M²
250
200
150
100
50
−50
−50
50
100
150
200
250
Ho W/M²

Fig 19

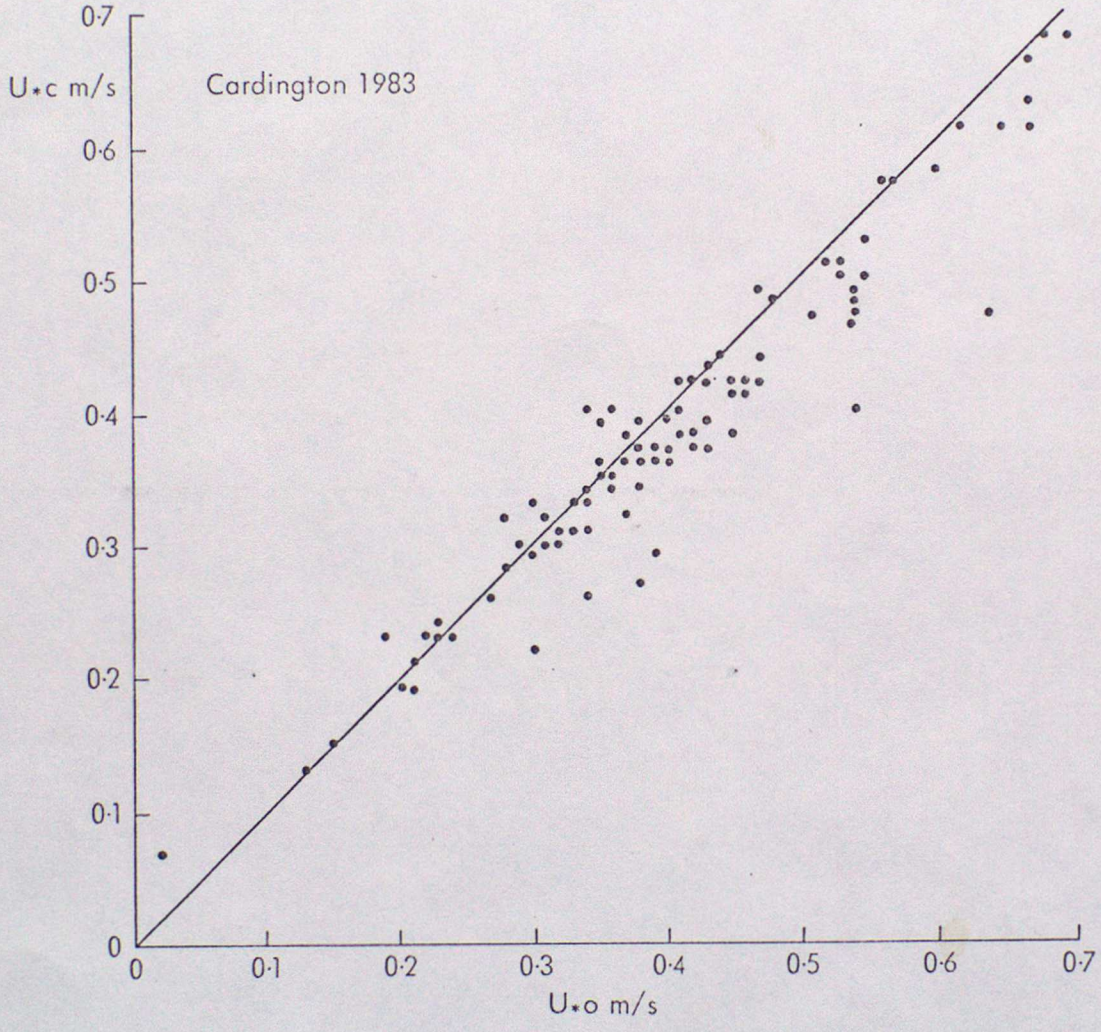
Cardington 1983
U*c m/s
U*o m/s
0·7
0·6
0·5
0·4
0·3
0·2
0·1
0
0
0·1
0·2
0·3
0·4
0·5
0·6
0·7